4.2.2 Dynamic Mechanical Thermal Analysis (DMTA) and Differential Scanning Calorimetry (DSC)

Dynamic mechanical thermal analysis or DMTA has been known as a well established method for studying the viscoelastic properties of polymer blends. From the DMTA measurements conducted over a wide range of temperature, it is possible to calculate the storage modulus (E'), loss modulus (E") as well as the mechanical loss factor or damping (tan δ) in dependence on temperature and deformation frequency. The storage modulus (E') is a measure of the energy stored and recovered per cycle and basically it determines a specimen's relevant stiffness. The purpose of loss factor or tan δ is to discern the various transition peaks occurring in each polymer blend and whether these peaks shift as a function of temperature. In this study, the DMT analyses were done on two categories of polymer blend that are the PVA blended with different concentration of different starches and PVA blended with different starches and mix with different concentrations of different treated fibers. The melting temperature or T_m of the polymer blends was determined by means of DSC. In the thermal-mechanical measurement through DMA analysis, the storage modulus (E'') and the loss factor (tan δ) for PVA incorporated with different concentrations of starch and treated fibers were evaluated.

The determination of an important parameter in the polymer blend, the glass transition temperature, T_g, was done using DMTA and not by the DSC method. This is partly because in polymer composites which are highly reinforced with natural fillers, the determination of T_g by means of DSC becomes very difficult as the specific heat capacity of the samples is only slightly changed by the glass transition but the weak glass transition can be determined more precisely using DMTA due to its higher sensitivity to changes in the heat capacity (Wielage, Lampke, Utschick, & Soergel, 2003) (Averous & Boquillon, 2004). In DMTA, the glass transition temperature is

generally associated with the tan δ peak position or with the onset temperature of the storage modulus drop both observed in the DMTA spectra (Cuq, Gontard, & Guilbert, 1997) (Ogale, Cunningham, Dawson, & Acton, 2000). It should also be noted that according to literature, the T_g obtained from DMTA was always higher than the T_g obtained using DSC method. This difference in T_g values may be because in DMTA analysis, the samples is heated in an open environment, allowing moisture to escape and this partly increases the T_g value (Mao, Imam, Gordon, Cinelli, & Chiellini, 2002).

Pure sample (PVA)

Figure 4.111 and 4.112 show the variation of the tensile storage modulus (E') and loss factor (tan δ) at 1 Hz as a function of temperature for pure PVA films. The melting temperature, T_m for pure PVA is shown in the DSC thermogram in Figure 4.113.

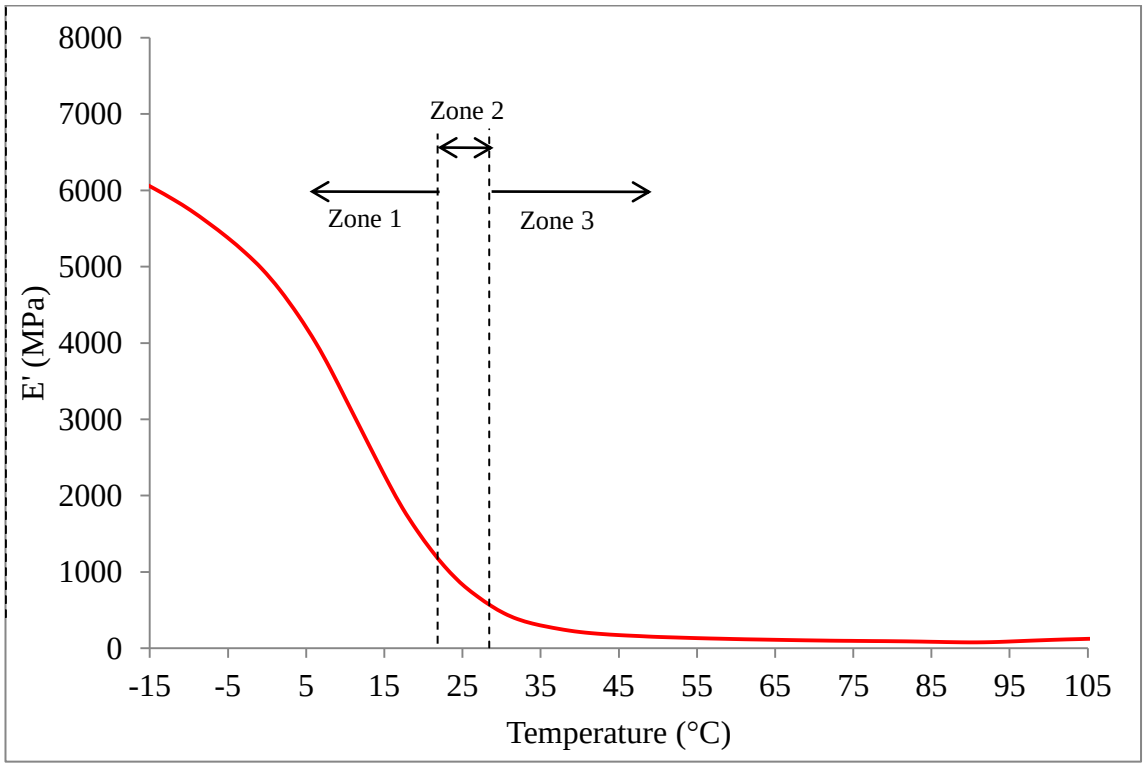

Fig. 4.111 Storage modulus (E') versus temperature at 1 Hz for pure PVA in film form

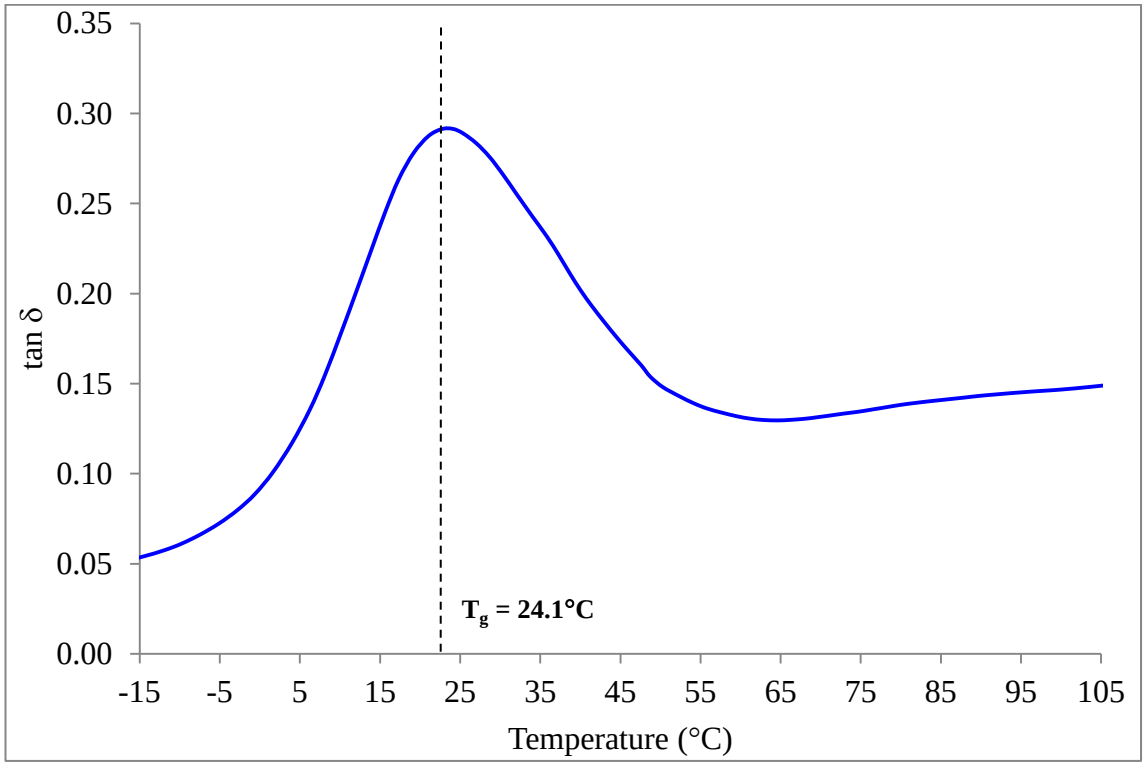

Fig. 4.112 tan δ versus temperature at 1 Hz for pure PVA in film form

For pure PVA, the variation in the storage modulus values in Figure 4.111 displays a typical behaviour of a semicrystalline polymer with three distinct zones. In the glassy state, the zone below the glass transition temperature (Zone 1), the storage modulus E' decreases with increasing temperature. This may be due to the increase in the segmental mobility of the polymer chains. Then, the modulus drops at the glass transition temperature, a temperature that depends on the moisture conditions of the specimen. PVA with its many hydrophilic groups exhibits a high affinity for substances containing hydroxyl groups. Adsorbed water plays a strong influence on the properties of hydrophilic polymers such as PVA. Water influences the structure of the polymer chain by acting as a plasticizer of the amorphous regions, and the properties of PVA in particular the glass transition temperature can be lowered substantially due to the

increase in the mobility of individual polymer chains (Chartoff, 1997). During the glass transition temperature zone (Zone 2), only the amorphous part of PVA undergoes segmental motion, while the crystalline portion remains solid until its melting temperature. After the glass transition zone (Zone 3), the amorphous rubbery domains coexist with the crystalline domains in the polymer matrix. From the observation on the tan δ versus temperature thermogram, it can be determined that the T_g of pure PVA in film form is 24.1°C. This value is substantially lower than reported in literature that is around 79-86°C because of the high moisture content in the film (Park, Park, & Ruckenstein, 2001) (Mao, Imam, Gordon, Cinelli, & Chiellini, 2002).

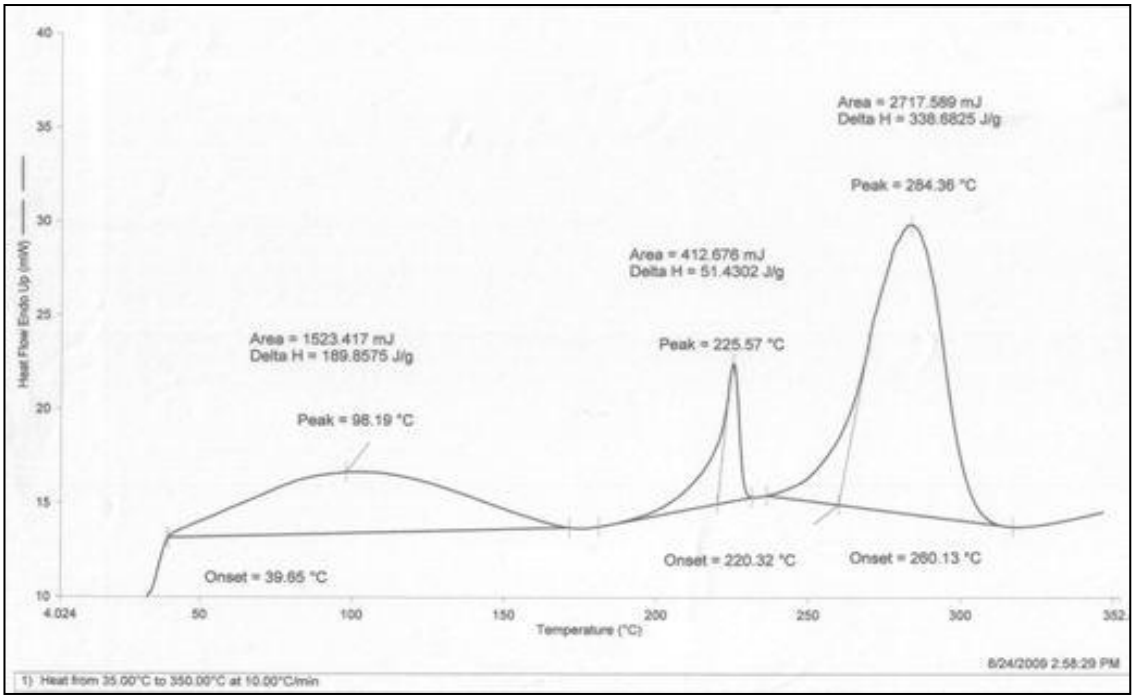

Fig. 4.113 DSC thermogram for pure PVA in film form

In the sample preparation process, the films of pure PVA and PVA blended with different concentration of starches and fibers were not completely dried as to prevent cracking and other changes in the properties of the blended films. High dehydration can

induce irreversible changes in the properties of the blended samples and thus it is avoided (Chielini, Cinelli, Fernandes, Kenawy, & Lazzeri, 2001).

In the thermal evaluation through DSC analysis, pure PVA exhibited three endothermic events, first at T = 98.19°C, and second at T = 225.57°C and the third at T = 284.36°C, respectively. It should be noted that the final endothermic peak observed from the DSC thermogram is the decomposition temperature for pure PVA as confirmed by thermogravimetric analysis result for pure PVA in Section 4.2.1. The second endothermic profile observed from the thermogram, at T = 225.57°C is the melting temperature, T_m for pure PVA. From the thermogram, the first endothermic event that occurred at T = 98.19°C has a higher change of enthalpy for the endothermic transition than the endothermic transition for the melting temperature. This may be attributed to the relatively easy detachment of small molecules of bound water from the PVA molecular chain and as a whole produces more disorder due to easy mobility and this consequently leads to higher change in the value of entropy (Mukherjee, 2009). In general, it can be assumed that the endothermic peak was due to the crystalline melting which was formed between residue bound water molecules and the molecular chains of PVA via hydrogen bonding. When the PVA film was heated during the DSC scanning, the water molecules bounded to the polymer molecular chains got activated to overcome the activation energy barrier required for entrapped absorbed water molecules to get adsorbed through hydrogen bonding with the liberation of heat. The transition at T = 98.19°C, involving PVA and water is neither a pure glass transition nor a pure melting transition of PVA but some kind of gel-sol transition (Watase & Nishinari, 1989). In fact, this gel structure depends on the intercalation of the PVA molecular chain with bound water and accordingly the transition temperature value varies (Murase, Gonda, & Watanabe, 1986) (Dibbern-Brunneli & Atvars, 2000).

PVA/different starches composites

Figure 4.114 to 4.116 shows the storage modulus versus temperature, as evaluated by DMA measurements in tensile mode for PVA/different starch composites.

Figure 4.117 to 4.119 show the tan δ versus temperature as evaluated by DMTA measurements in tensile mode for PVA/different starch composites.

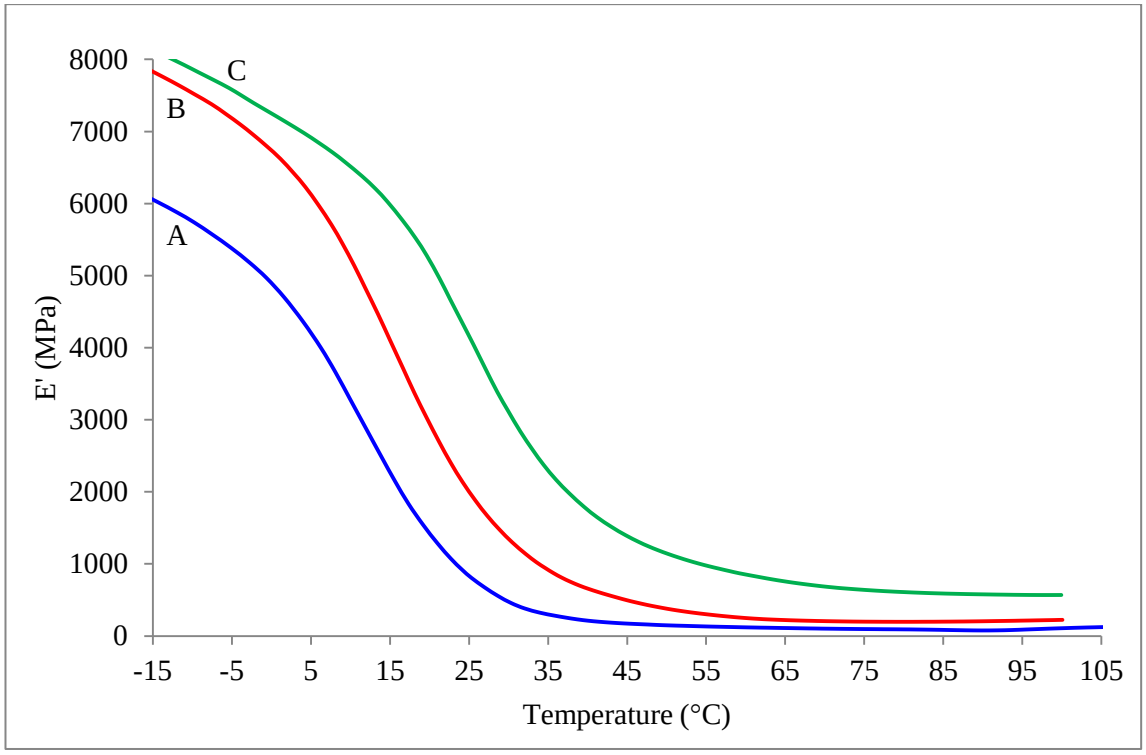

Fig. 4.114 Storage modulus (E') vs. temperature for PVA/1TS (B) and PVA/3TS (C) composites. The thermograms were compared with the DMA thermogram for pure PVA (A).

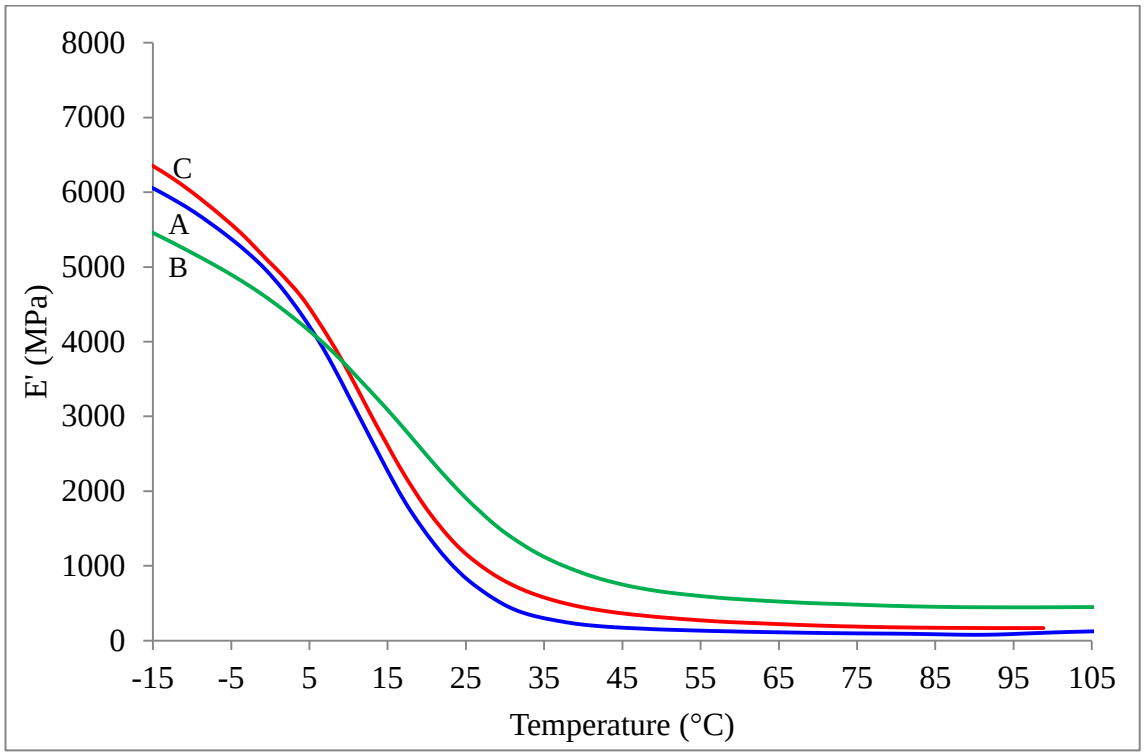

Fig. 4.115 Storage modulus (E') vs. temperature for PVA/1RS (C) and PVA/3RS (B) composites. The thermograms were compared with the DMA thermogram for pure PVA (A).

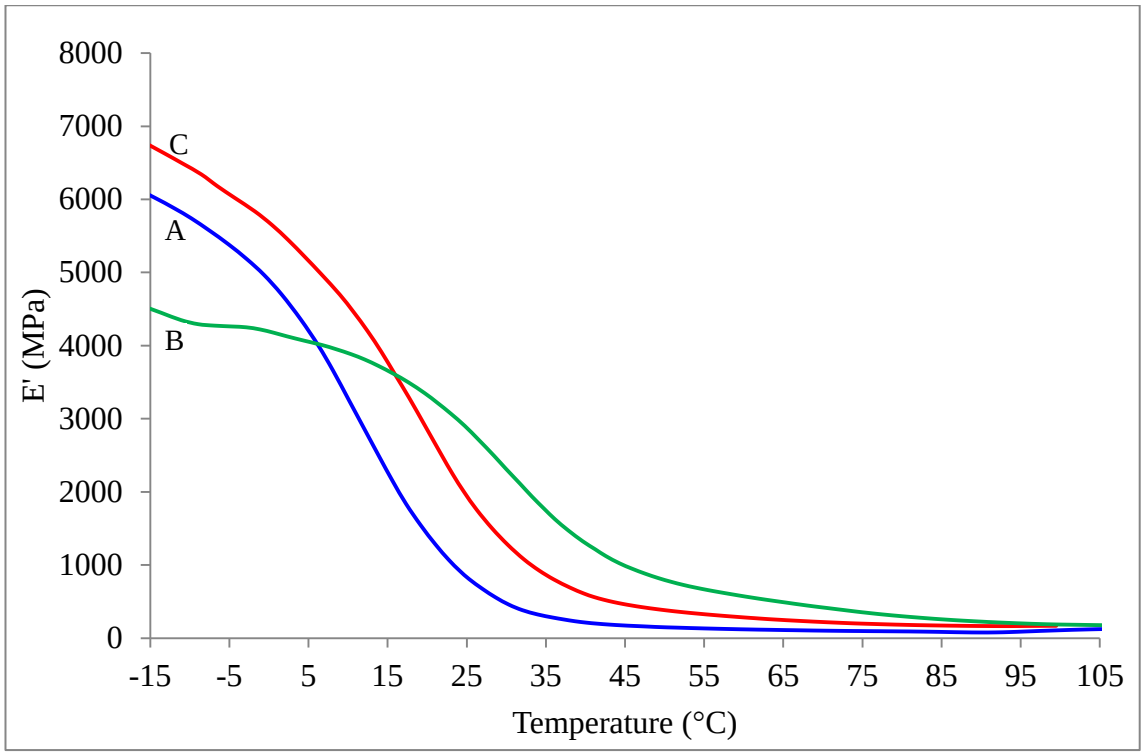

Fig. 4.116 Storage modulus (E') vs. temperature for PVA/1SS (C) and PVA/3SS (B) composites. The thermograms were compared with the DMA thermogram for pure PVA (A).

In general, from the thermograms of storage modulus vs. temperature for PVA blended with different concentration of different starches, the composites with higher concentration of starches exhibit an increase in the storage modulus at temperatures higher than the glass transition temperature. This phenomenon may be contributed by the strong interfacial interaction through hydrogen bonding between starch and the PVA matrix. As an example from Figure 4.114, the storage modulus of the composites filled with 3g of tapioca starch is about 8 times higher than that of pure PVA film at 35°C, indicating a higher thermal stability of the resulting composites. It can also be seen that from the thermograms, as the temperature increases, the E' values for all the composites decreases up to a point (around 75°C) where the E' values plateau's off. This event may be attributed to softening of the polymer matrix at high temperatures.

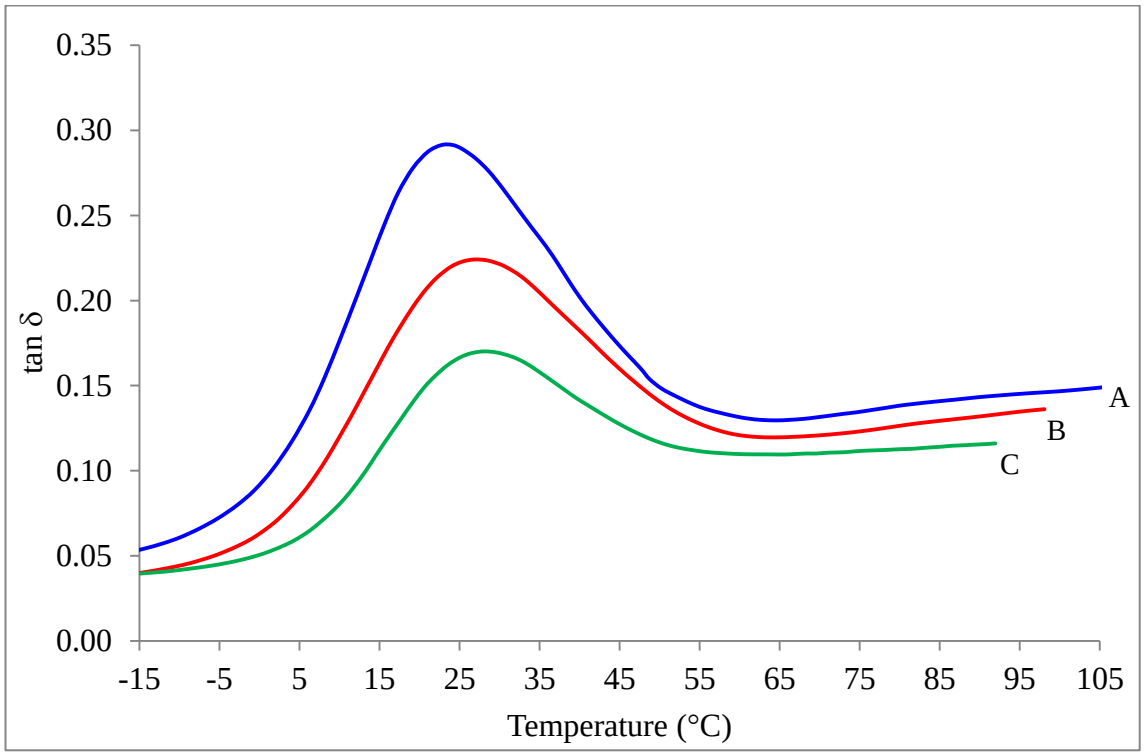

Fig. 4.117 Loss factor (tan δ) vs. temperature for PVA/1TS (C) and PVA/3TS (B) composites. The thermograms were compared with the DMA thermogram for pure PVA (A).

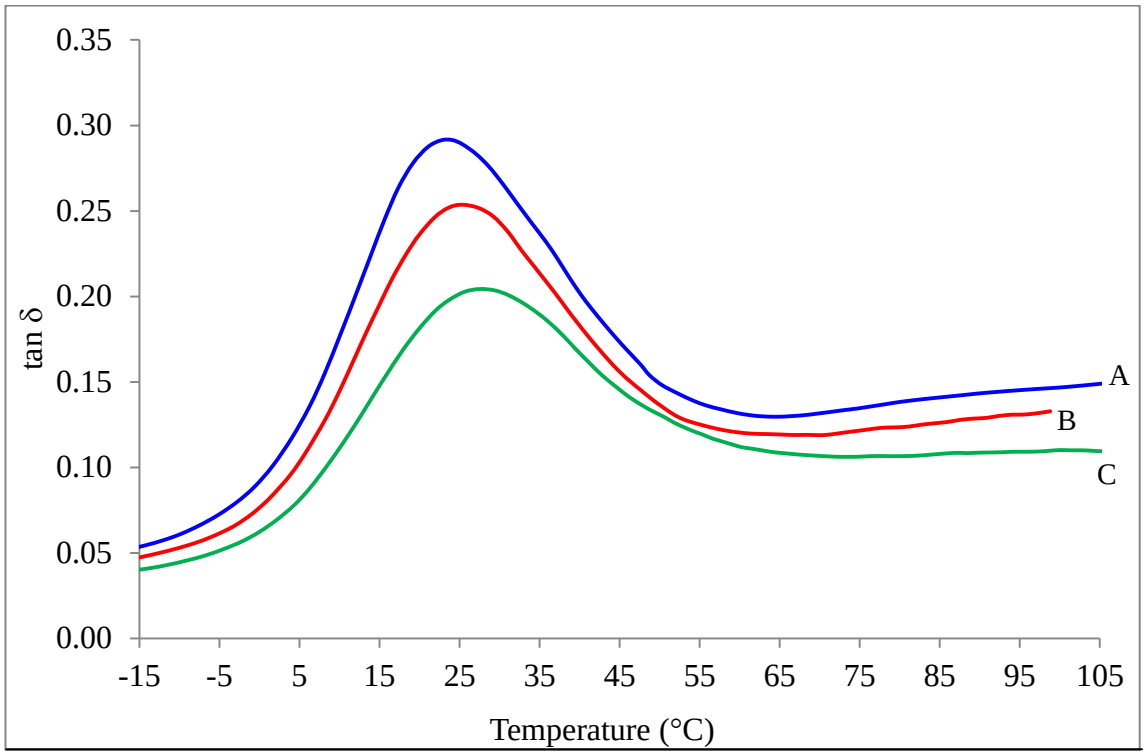

Fig. 4.118 Loss factor (tan δ) vs. temperature for PVA/1RS (C) and PVA/3RS (B) composites. The thermograms were compared with the DMA thermogram for pure PVA (A).

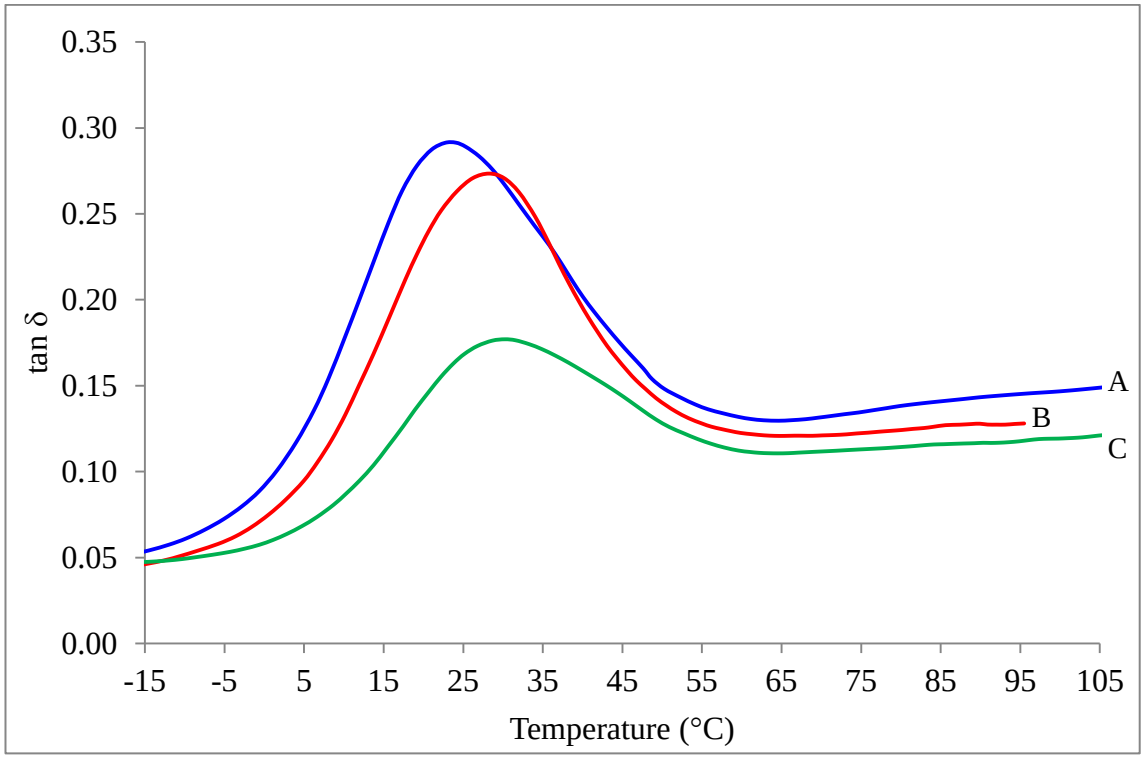

Fig. 4.119 Loss factor (tan δ) vs. temperature for PVA/1SS (C) and PVA/3SS (B) composites. The thermograms were compared with the DMA thermogram for pure PVA (A).

From the observation on the thermograms of tan δ versus temperature for all the blends of PVA with different starches (Figure 4.117 – 4.119), the glass transition temperature obtained from the tan δ peak position slightly increased as the concentration of starch in the blend increases. This may indicate that there are restrictions in the molecular motion of starch and PVA molecules, and may be due to the strong interaction between different starch and the polymer matrix especially between linkages through hydrogen bonding in the blend. A decrease in magnitude for the tan δ values upon addition of different concentration of starches was also observed, and this suggests that there are good interfacial adhesion between starch and the polymer matrix. The reason for this behaviour may be because of the limited mobility of the polymeric molecular chain due to the interactions between starch and matrix. As the temperature increases, it is also noted that the composites blended with starches showed a broader peak than the pure PVA matrix. The peak of tan δ gets broader as the concentration of starch in the blend increases. The broadening of the loss modulus peak may be due to the increase in the energy absorption by the components in the blended films. Table 4.9 lists down the glass transition temperature, T_g for the composites of PVA blended with different concentration of different starches.

Table 4.9 The glass transition temperature, T_g for PVA blended with different concentration of different starches

	T_g (°C)		**T_g (°C)**		**T_g (°C)**
PVA	24				
PVA/1TS	25	PVA/1RS	25	PVA/1SS	28
PVA/3TS	28	PVA/3RS	28	PVA/3SS	30

PVA/different starches/different fibers composites

Table 4.10 shows the list of all the glass transition temperature, T_g and the melting temperature, T_m for all the PVA/starches/fibers blended samples.

Figure 4.120 to 4.127 shows the DSC thermograms for PVA blended with 1g of tapioca starch and mix with different concentration of different treated fibers.

Figure 4.128 to 4.135 shows the DSC thermograms for PVA blended with 1g of rice starch and mix with different concentration of different treated fibers.

Figure 4.136 to 4.143 shows the DSC thermograms for PVA blended with 1g of sago starch and mix with different concentration of different treated fibers.

Table 4.10 The glass transition temperature, T_g and the melting temperature, T_m for the composites PVA blended with 1g of different starches and different concentration of different treated fibers.

Composites	T_g (°C)	T_m (°C)
PVA	24	226
PVA/1TS/1BB	32	227
PVA/1TS/3BB	37	223
PVA/1TS/1KF	31	225
PVA/1TS/3KF	37	225
PVA/1TS/1ROS	34	223
PVA/1TS/3ROS	35	224
PVA/1TS/1NP	30	224
PVA/1TS/3NP	33	220
PVA/1RS/1BB	27	228
PVA/1RS/3BB	31	223

PVA/1RS/1KF	28	225
PVA/1RS/3KF	31	224
PVA/1RS/1ROS	29	226
PVA/1RS/3ROS	31	222
PVA/1RS/1NP	30	222
PVA/1RS/3NP	33	221
PVA/1SS/1BB	31	226
PVA/1SS/3BB	32	221
PVA/1SS/1KF	29	224
PVA/1SS/3KF	32	225
PVA/1SS/1ROS	30	225
PVA/1SS/3ROS	36	222
PVA/1SS/1NP	31	223
PVA/1SS/3NP	33	220

From the T_g values listed, it can be deduced that there is an increase in the glass transition temperature dependence on the content of the treated fibers and this might be contributed by the occurrence of intermolecular interaction in the interfacial zone between PVA, starch and the treated fiber's stiff crystallites. This also implies that the cellulosic fibers are physically encapsulated by the melted PVA matrix and physically inhibits the mobilization of the PVA molecular chain (Yang, Gardner, & Kim, 2009). The shifting of the glass transition temperature in the blended films also suggests that the thermal stability and deflection resistance of the composites increased with increasing concentration of treated fiber content. This finding can be supported by the thermograms of PVA incorporated with different starches and blended with different

concentration of treated fibers in section 4.2.1. It can also be observed that as the content of the treated fibers incorporated in the composite increases, there is a depression in the melting temperature. This basically indicates that the ordered association of the PVA molecules in the blended films was decreased by the presence of cellulose fibers. The melting temperature depression also suggests that the PVA molecules were highly constrained by the entanglement of PVA, starch and cellulose molecules. The entanglement of different components that make up the blend suggests that strong interaction exists between the cellulosic fiber's surface and the polymeric matrix. These interactions most probably restrict the capability of the matrix chains to form big crystalline domains (Roohani, Habibi, Belgacem, Ebrahim, Karimi, & Dufresne, 2008). The incapability of the composite to form big crystalline domains may be related to the decrease in crystallite size due to the formation of a close cellulose network within the polymer matrix and this is supported by calculated crystallite width for polymer blended with different concentrations of cellulosic fiber from the XRD diffractograms in section 4.2.

Figure 4.144 to 4.147 shows the storage modulus versus temperature, as evaluated by DMTA measurements in tensile mode for PVA blended with 1g of tapioca starch and mix with different concentration of different treated fibers.

Figure 4.148 to 4.151 shows the storage modulus versus temperature, as evaluated by DMTA measurements in tensile mode for PVA blended with 1g of rice starch and mix with different concentration of different treated fibers.

Figure 4.152 to 4.155 shows the storage modulus versus temperature, as evaluated by DMTA measurements in tensile mode for PVA blended with 1g of sago starch and mix with different concentration of different treated fibers

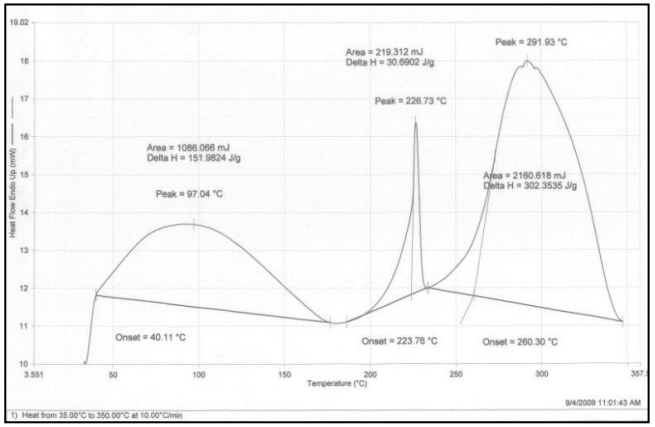

Fig.4.120 DSC thermogram for PVA/1TS/1BB

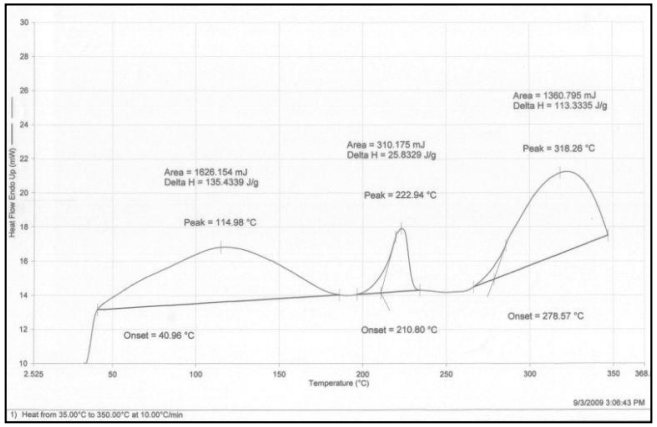

Fig 4.121 DSC thermogram for PVA/1TS/3BB

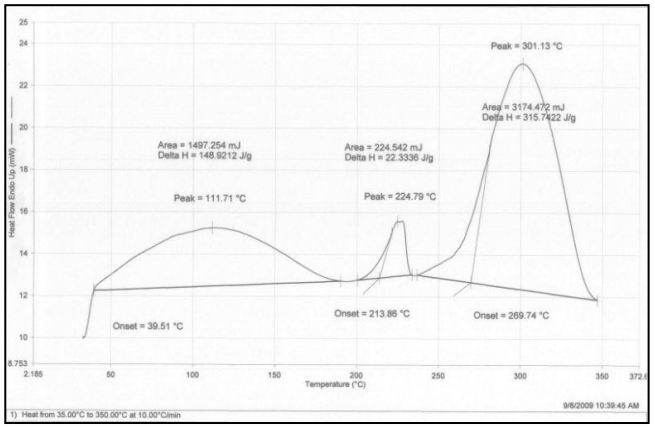

Fig. 4.122 DSC thermogram for PVA/1TS/1KF

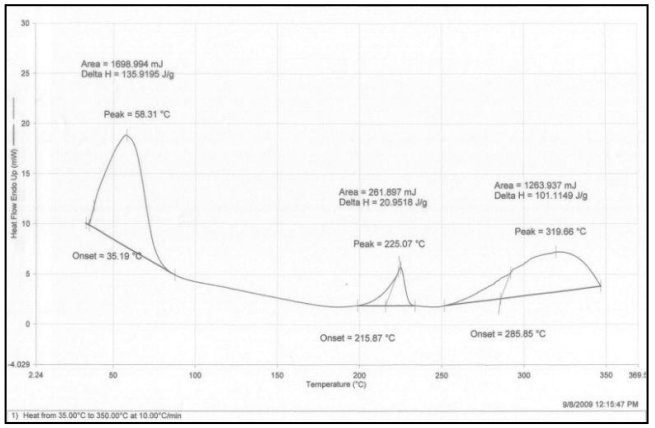

Fig. 4.123 DSC thermogram for PVA/1TS/3KF

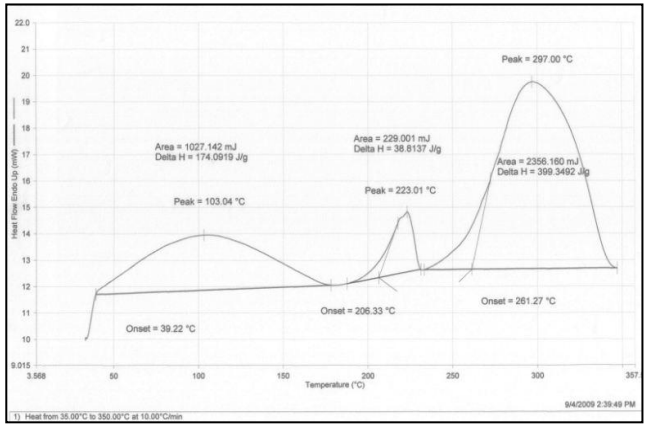

Fig. 4.124 DSC thermogram for PVA/1TS/1ROS

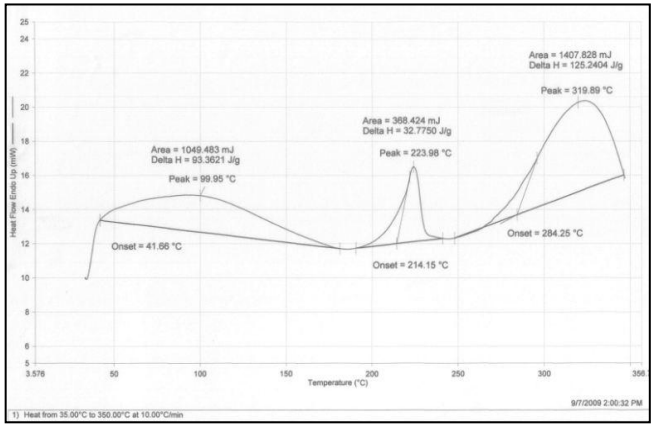

Fig. 4.125 DSC thermograms for PVA/1TS/3ROS

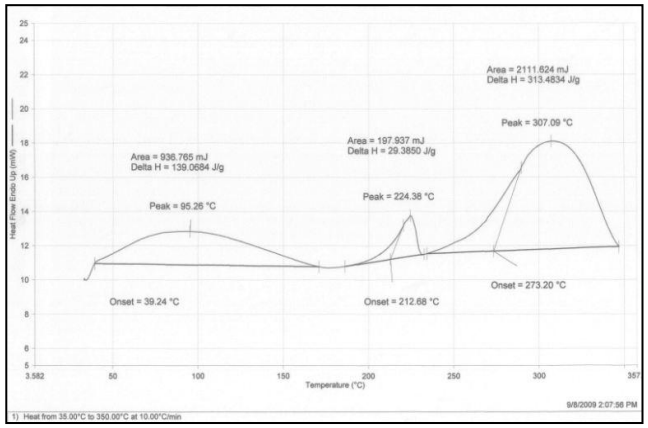

Fig. 4.126 DSC thermogram for PVA/1TS/1NP

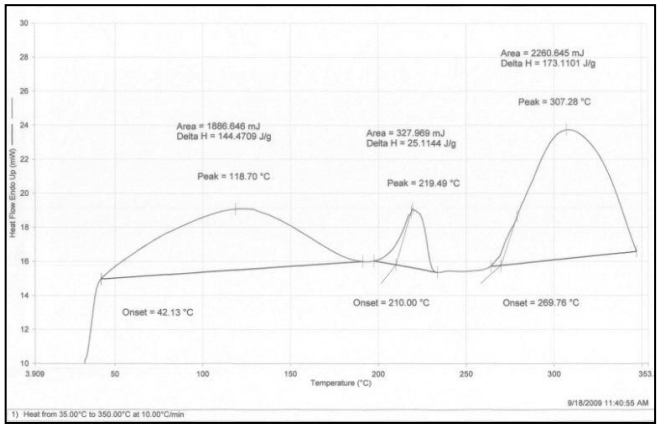

Fig. 4.127 DSC thermogram for PVA/1TS/3NP

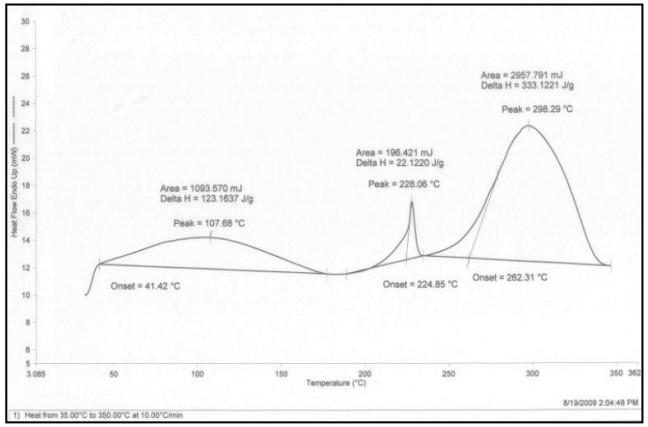

Fig. 4.128 DSC thermogram for PVA/1RS/1BB

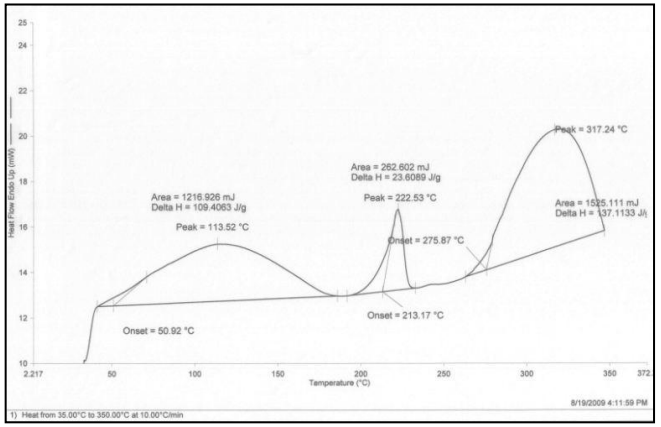

Fig. 4.129 DSC thermogram for PVA/1RS/3BB

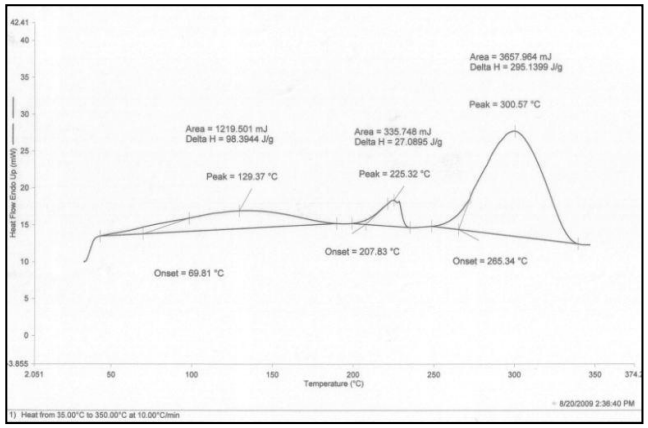

Fig. 4.130 DSC thermogram for PVA/1RS/1KF

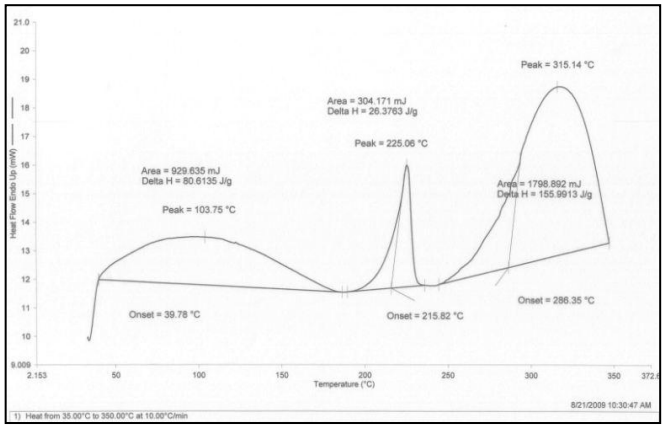

Fig. 4.131 DSC thermogram for PVA/1RS/3KF

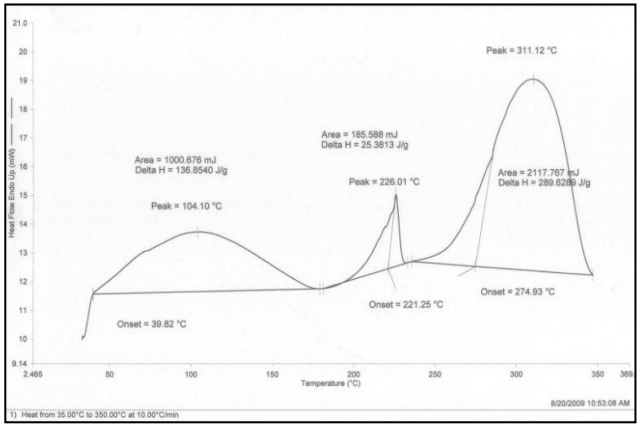

Fig. 4.132 DSC thermogram for PVA/1RS/1ROS

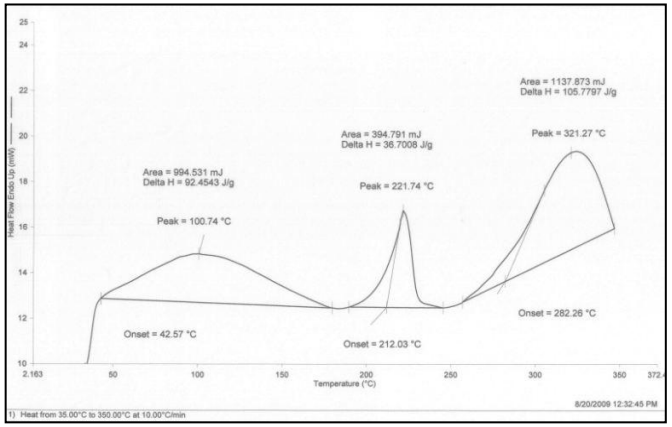

Fig. 4.133 DSC thermogram for PVA/1RS/3ROS

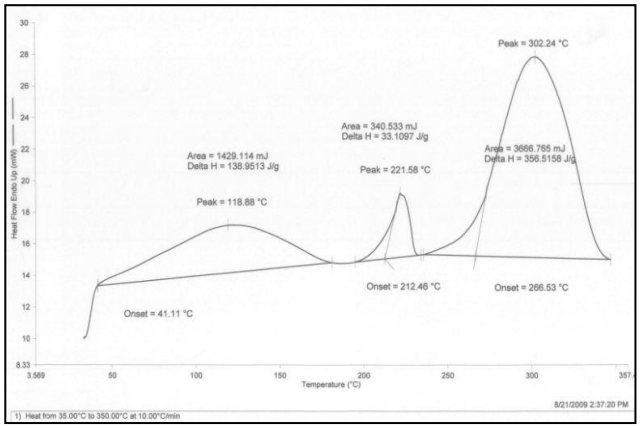

Fig. 4.134 DSC thermogram for PVA/1RS/1NP

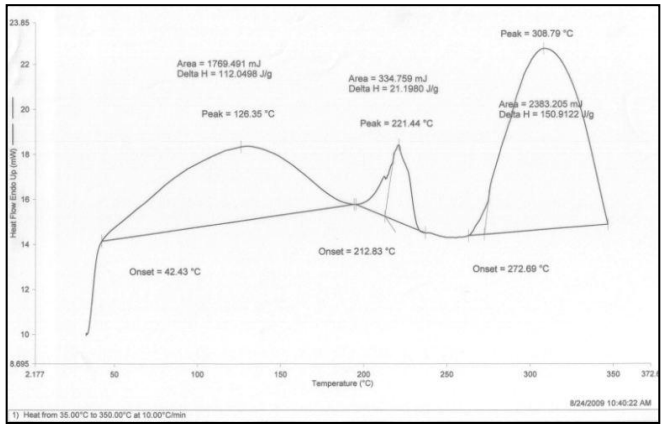

Fig. 4.135 DSC thermogram for PVA/1RS/3NP

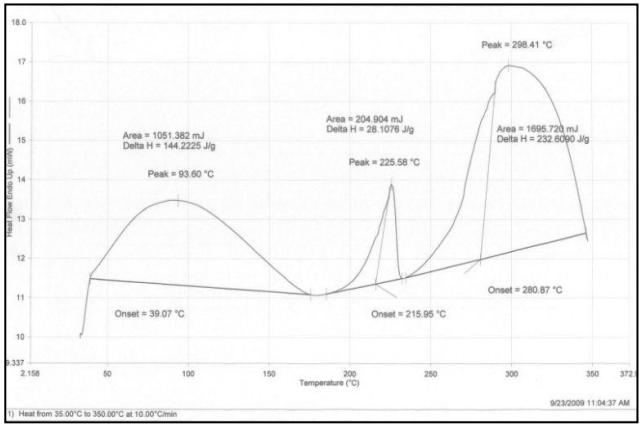

Fig. 4.136 DSC thermogram for PVA/1SS/1BB

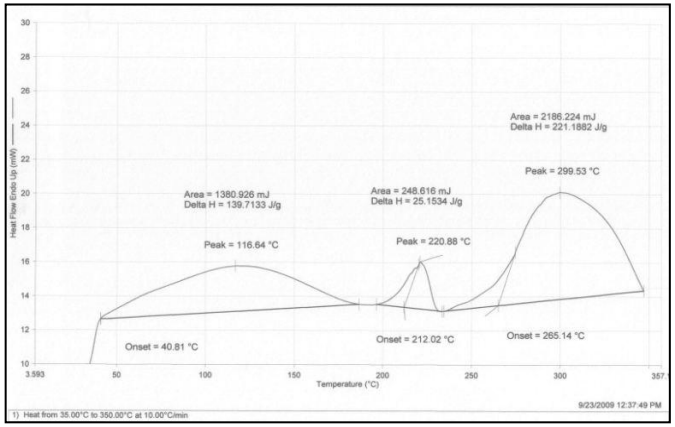

Fig. 4.137 DSC thermogram for PVA/1SS/3BB

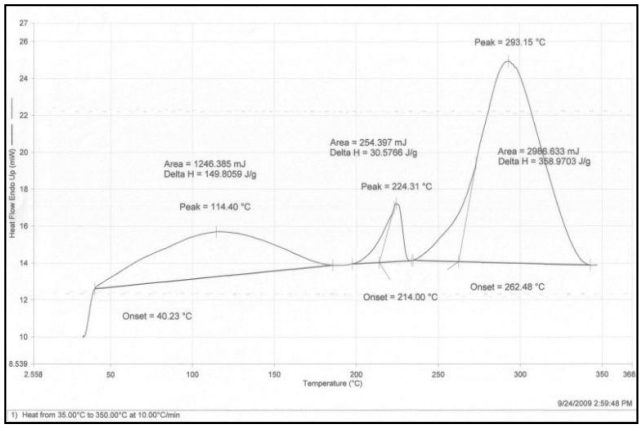

Fig. 4.138 DSC thermogram for PVA/1SS/1KF

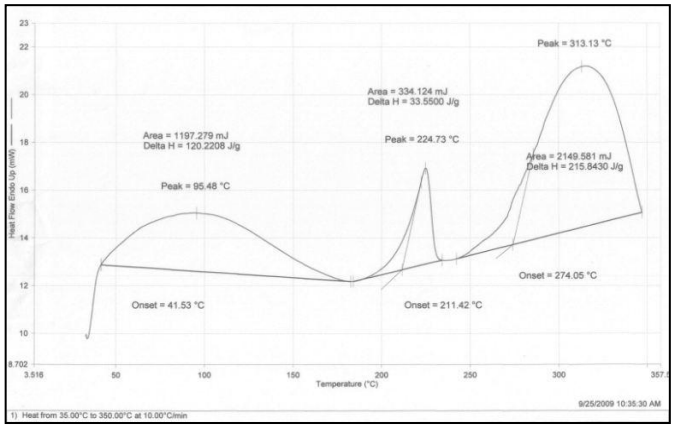

Fig. 4.139 DSC thermogram for PVA/1SS/3KF

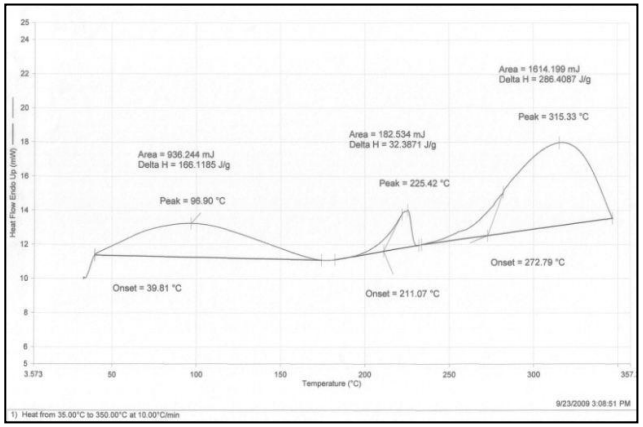

Fig. 4.140 DSC thermogram for PVA/1SS/1ROS

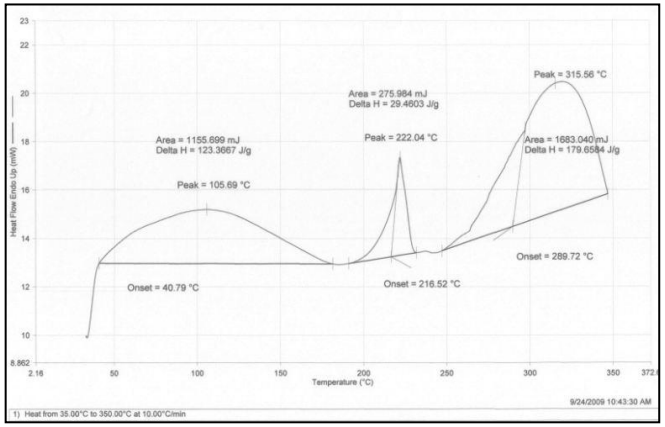

Fig. 4.141 DSC themorgram for PVA/1SS/3ROS

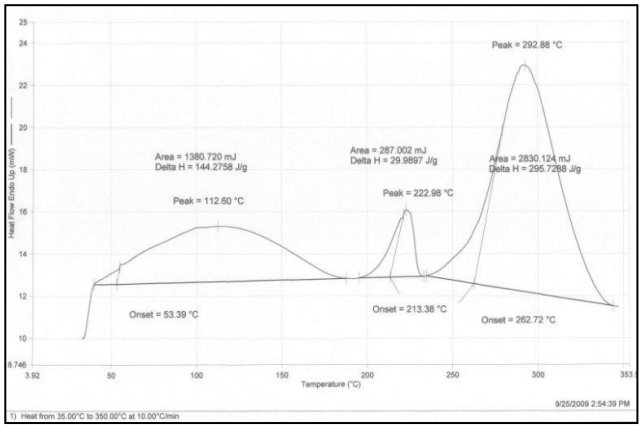

Fig. 4.142 DSC thermogram for PVA/1SS/1NP

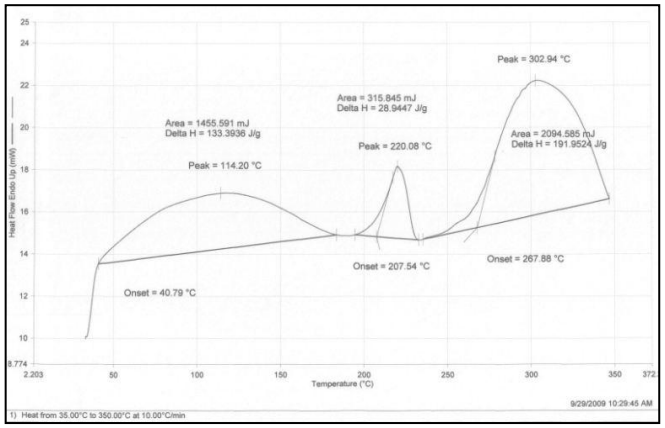

Fig. 4.143 DSC thermogram for PVA/1SS/3NP

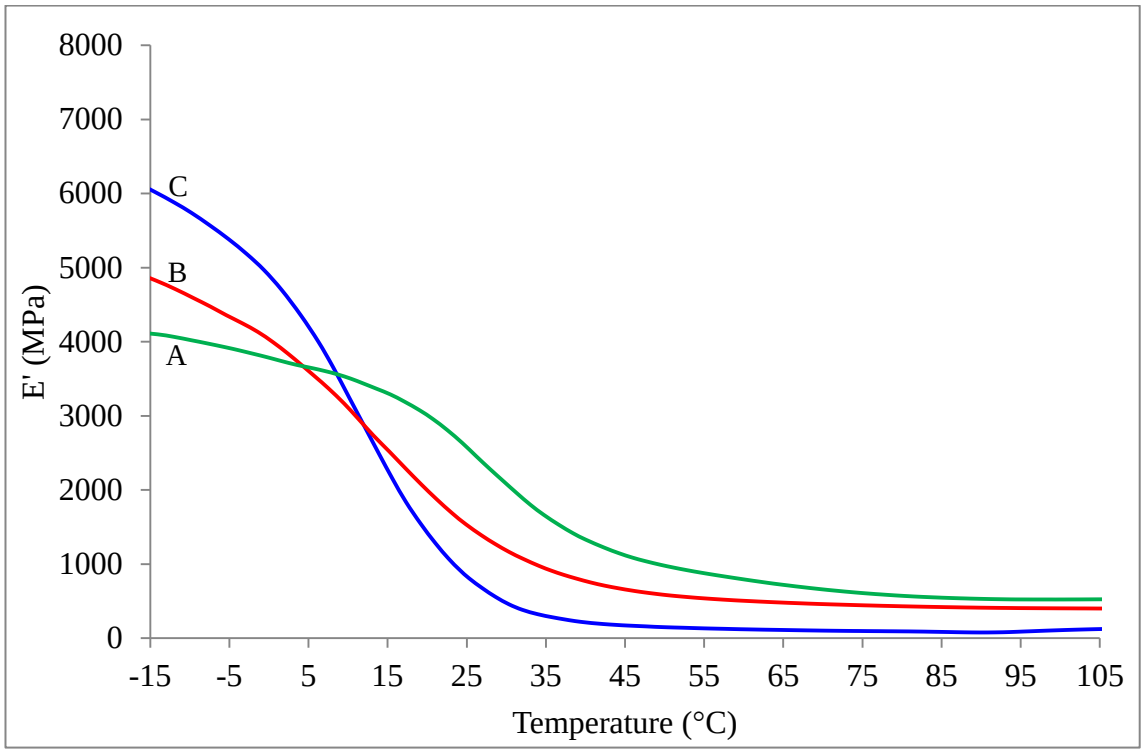

Fig. 4.144 Storage modulus (E') vs. temperature for PVA/1TS/1BB (B) and PVA/1TS/3BB (A) composites. The thermograms were compared with the DMA thermogram for pure PVA (C).

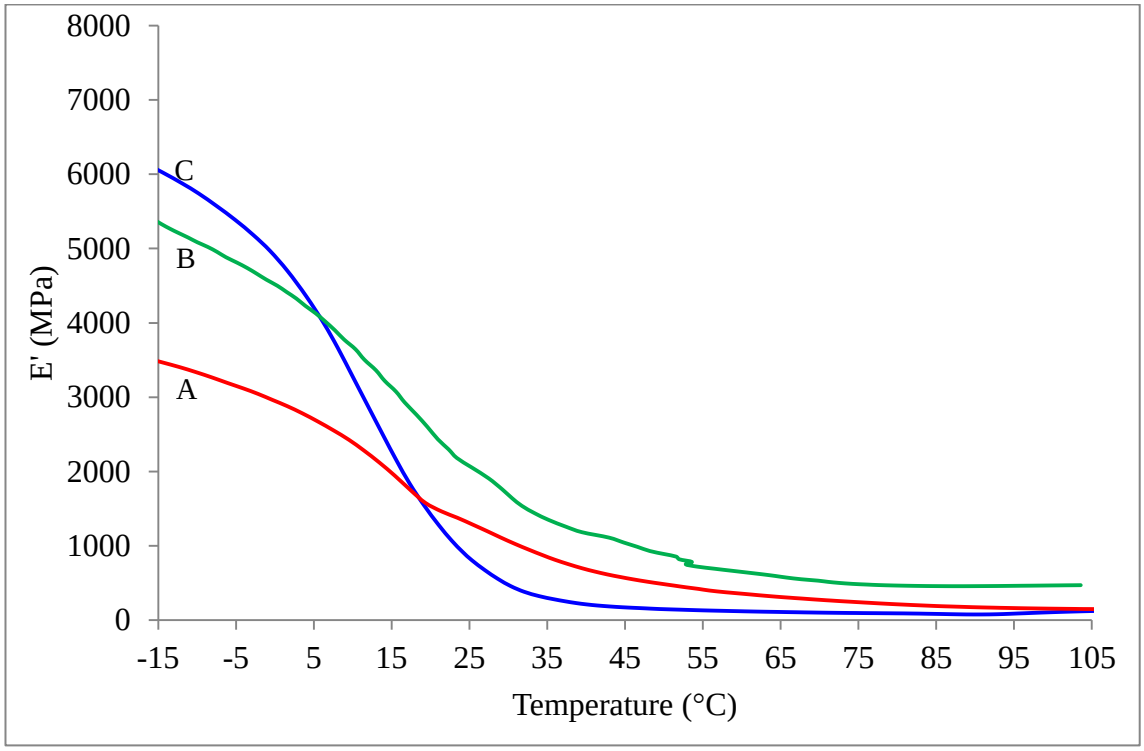

Fig. 4.145 Storage modulus (E') vs. temperature for PVA/1TS/1KF (A) and PVA/1TS/3KF (B) composites. The thermograms were compared with the DMA thermogram for pure PVA (C).

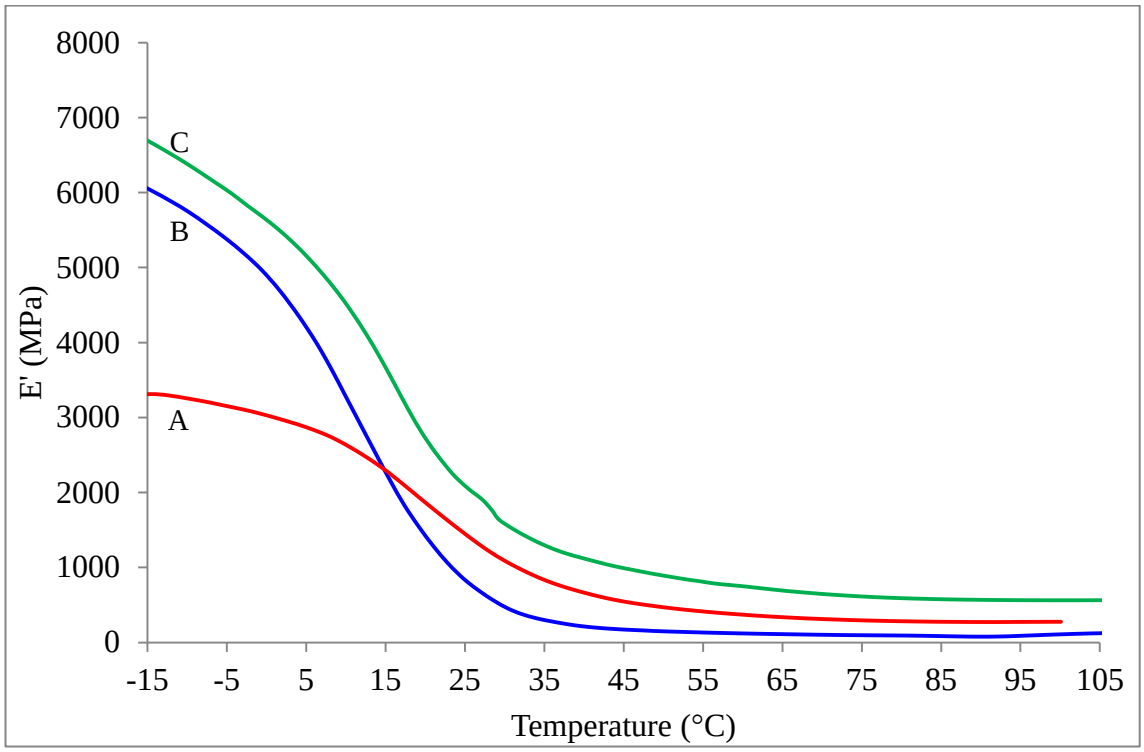

Fig. 4.146 Storage modulus (E') vs. temperature for PVA/1TS/1ROS (A) and PVA/1TS/3ROS (C) composites. The thermograms were compared with the DMA thermogram for pure PVA (B).

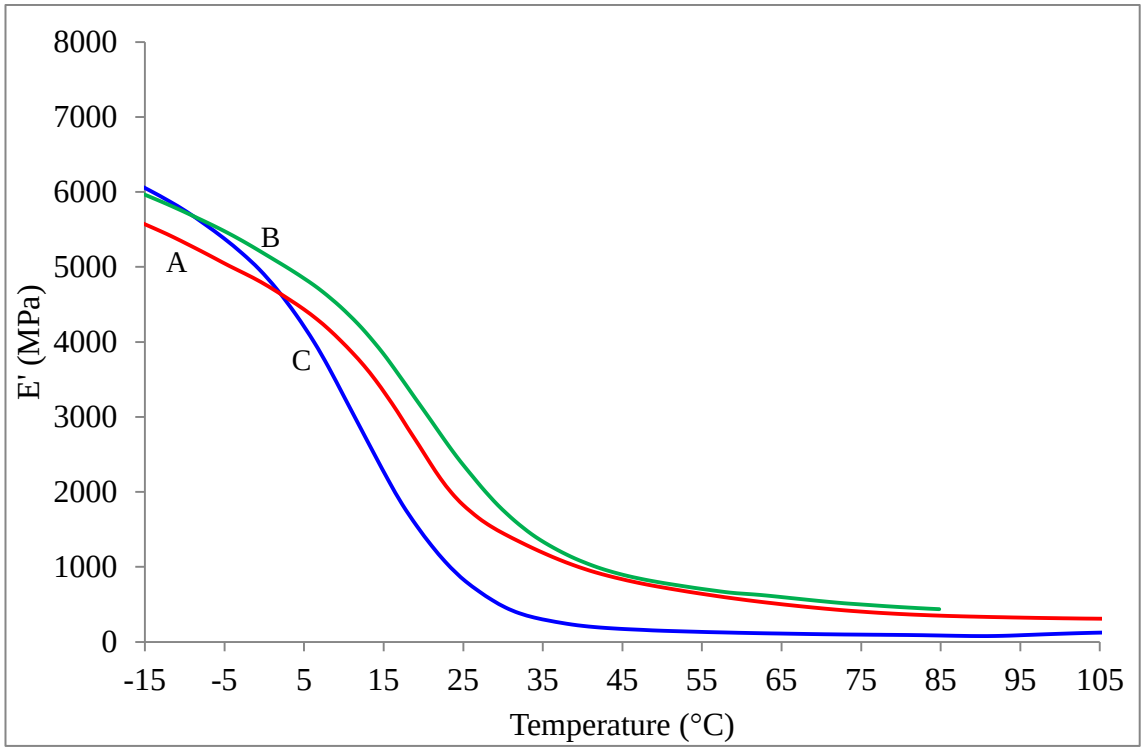

Fig. 4.147 Storage modulus (E') vs. temperature for PVA/1TS/1NP (A) and PVA/1TS/3NP (B) composites. The thermograms were compared with the DMA thermogram for pure PVA (C).

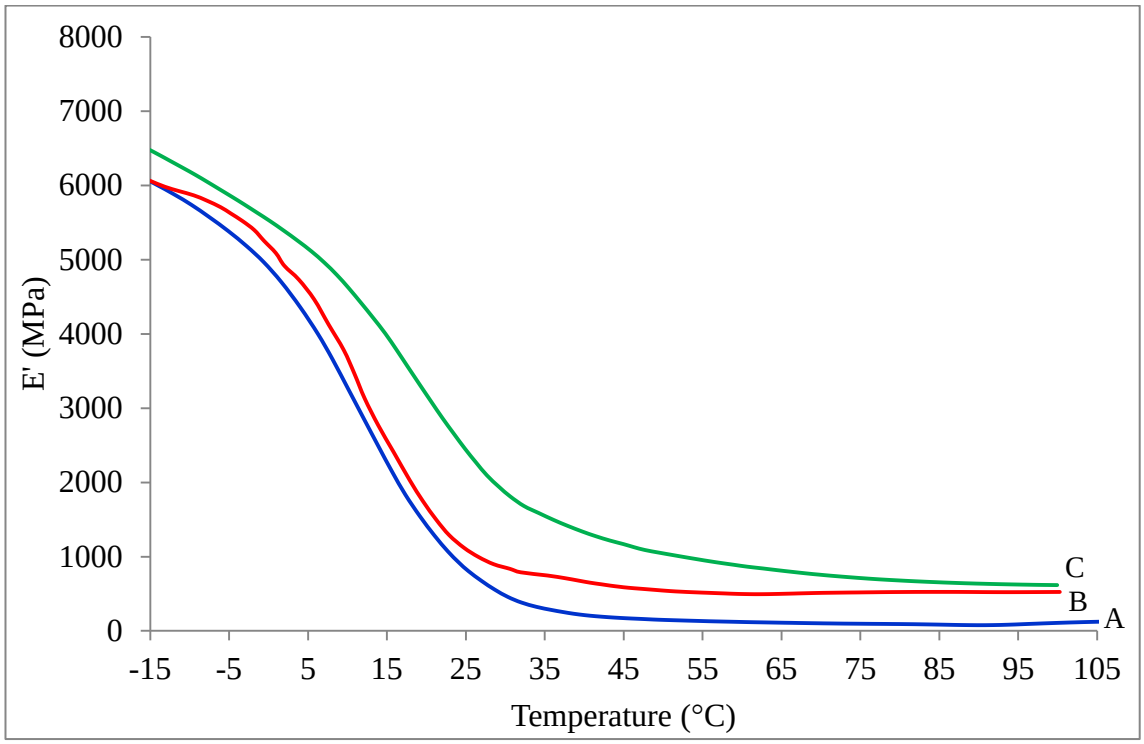

Fig. 4.148 Storage modulus (E') vs. temperature for PVA/1RS/1BB (B) and PVA/1RS/3BB (C) composites. The thermograms were compared with the DMA thermogram for pure PVA (A).

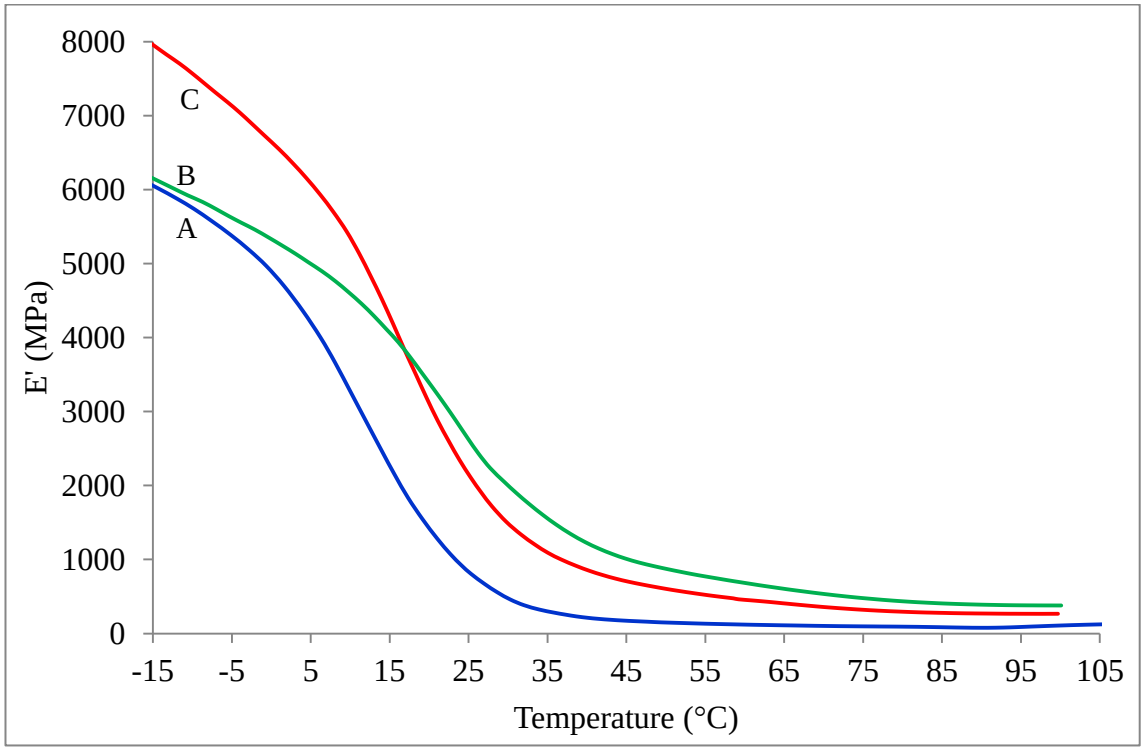

Fig. 4.149 Storage modulus (E') vs. temperature for PVA/1RS/1KF (C) and PVA/1RS/3KF (B) composites. The thermograms were compared with the DMA thermogram for pure PVA (A).

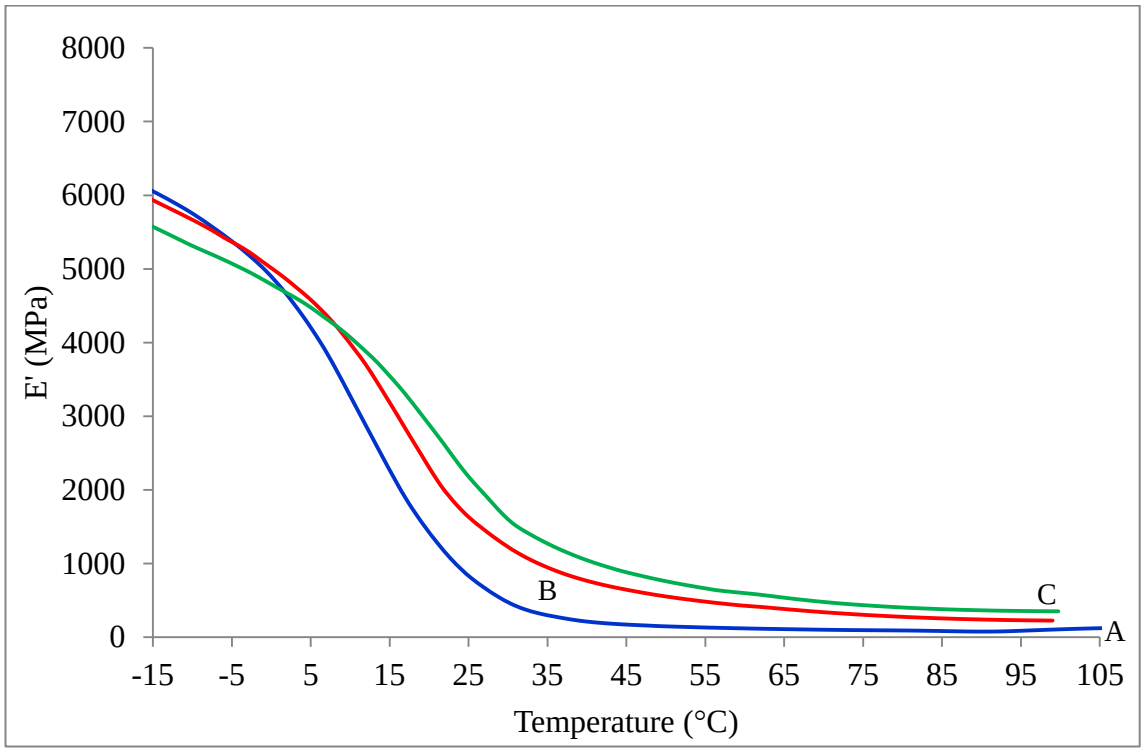

Fig. 4.150 Storage modulus (E') vs. temperature for PVA/1RS/1ROS (B) and PVA/1RS/3ROS (C) composites. The thermograms were compared with the DMA thermogram for pure PVA (A).

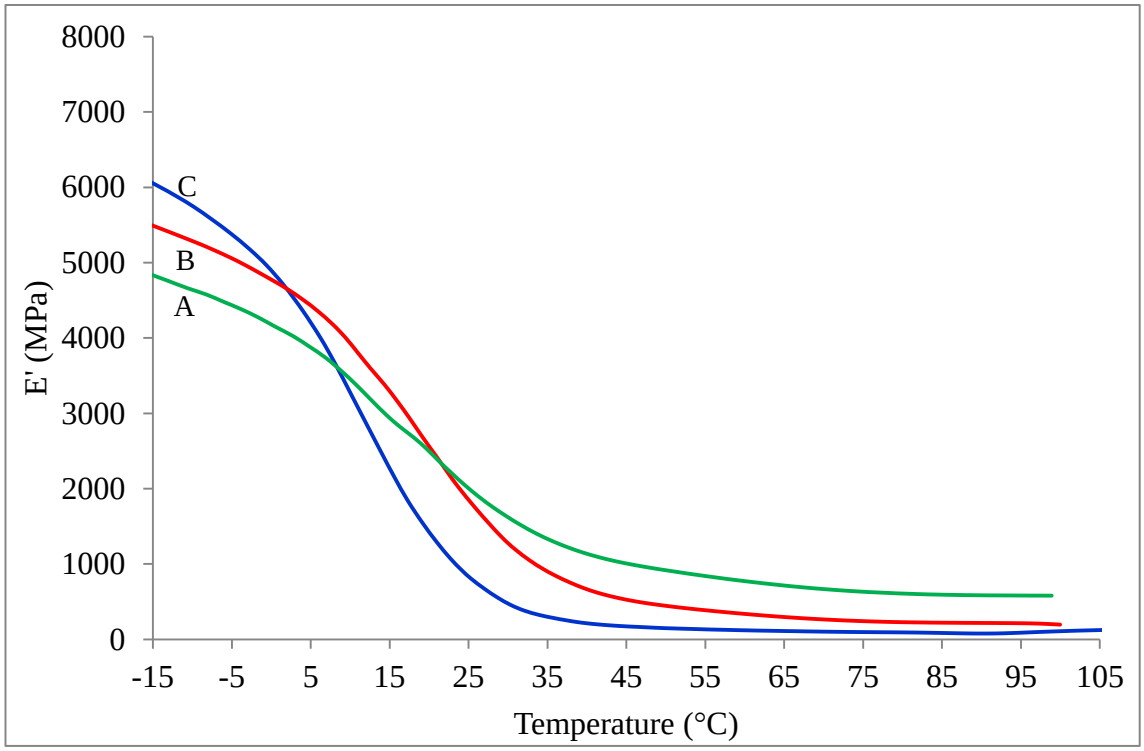

Fig. 4.151 Storage modulus (E') vs. temperature for PVA/1RS/1NP (B) and PVA/1RS/3NP (A) composites. The thermograms were compared with the DMA thermogram for pure PVA (C).

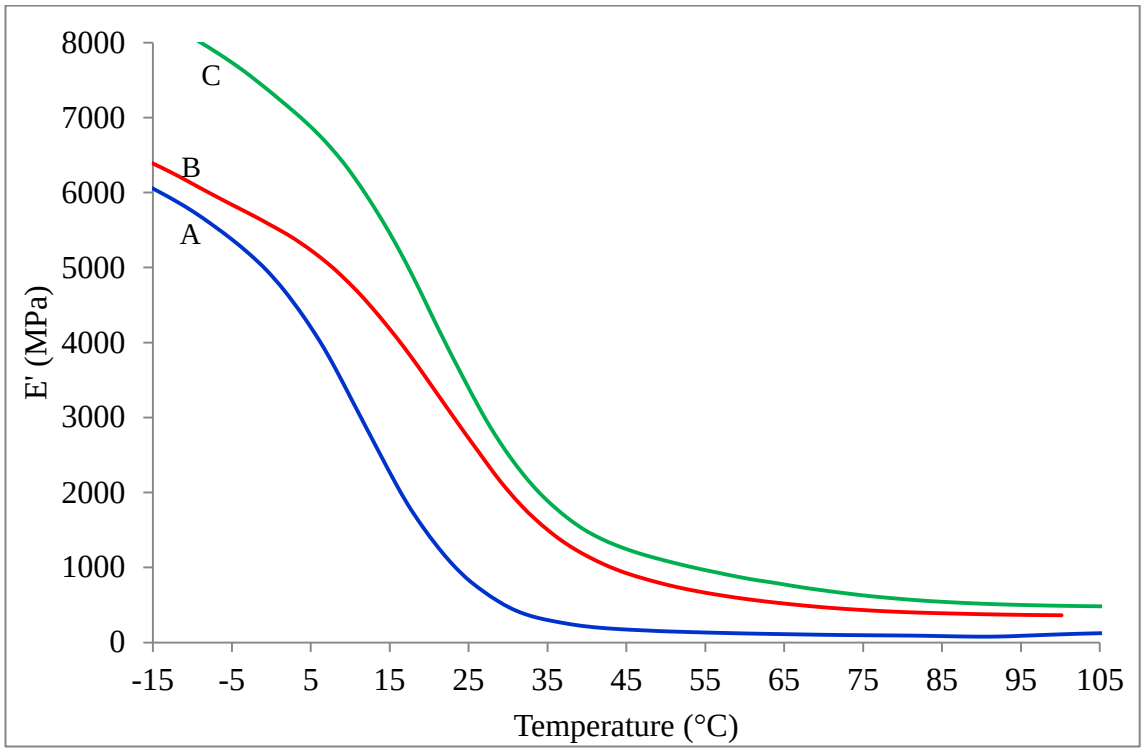

Fig. 4.152 Storage modulus (E') vs. temperature for PVA/1SS/1BB (B) and PVA/1SS/3BB (C) composites. The thermograms were compared with the DMA thermogram for pure PVA (A).

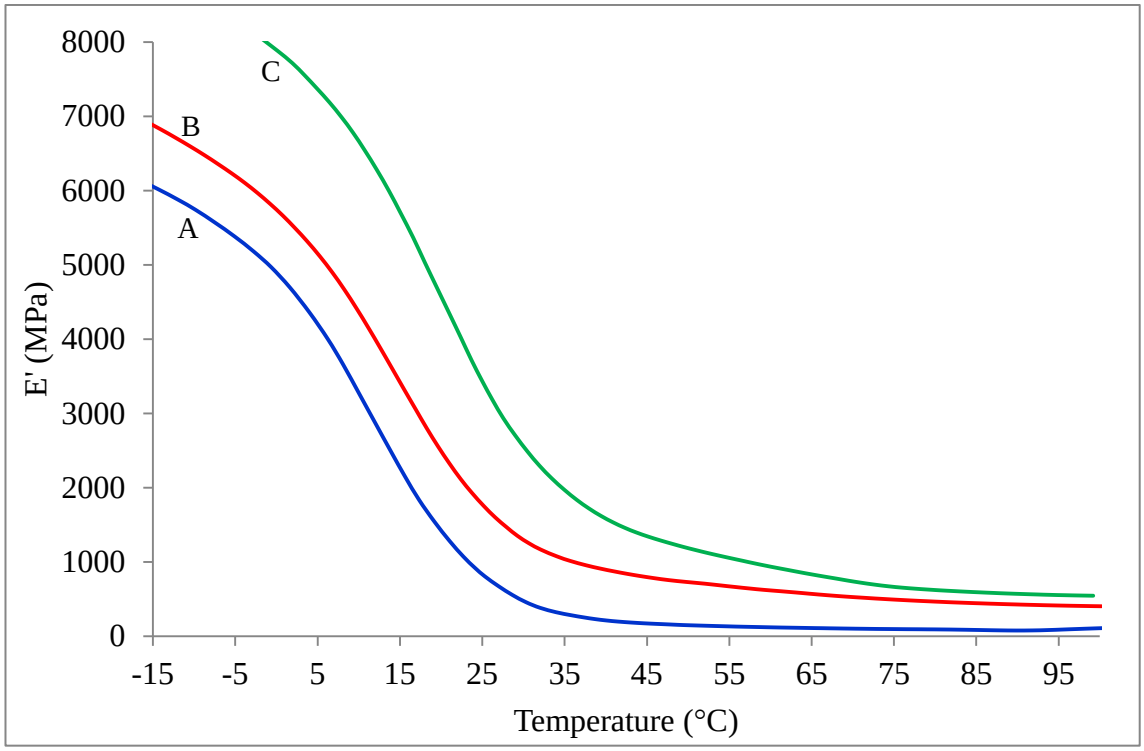

Fig. 4.153 Storage modulus (E') vs. temperature for PVA/1SS/1KF (B) and PVA/1SS/3KF (C) composites. The thermograms were compared with the DMA thermogram for pure PVA (A).

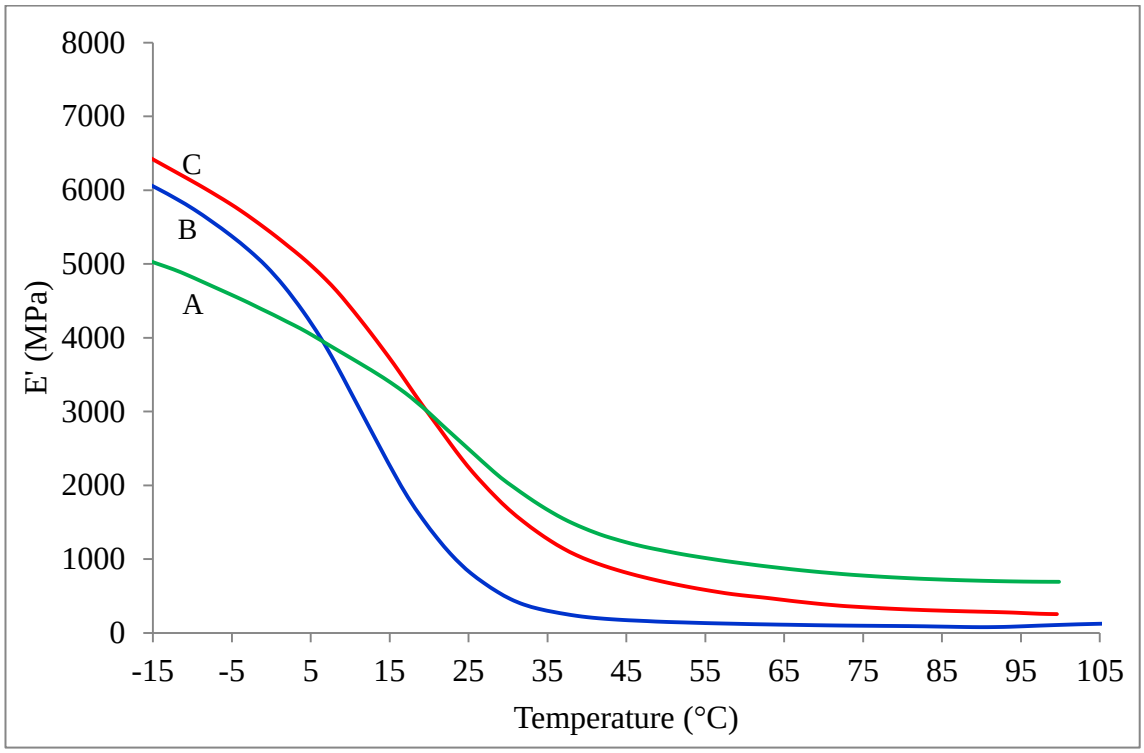

Fig. 4.154 Storage modulus (E') vs. temperature for PVA/1SS/1ROS (B) and PVA/1SS/3ROS (C) composites. The thermograms were compared with the DMA thermogram for pure PVA (A).

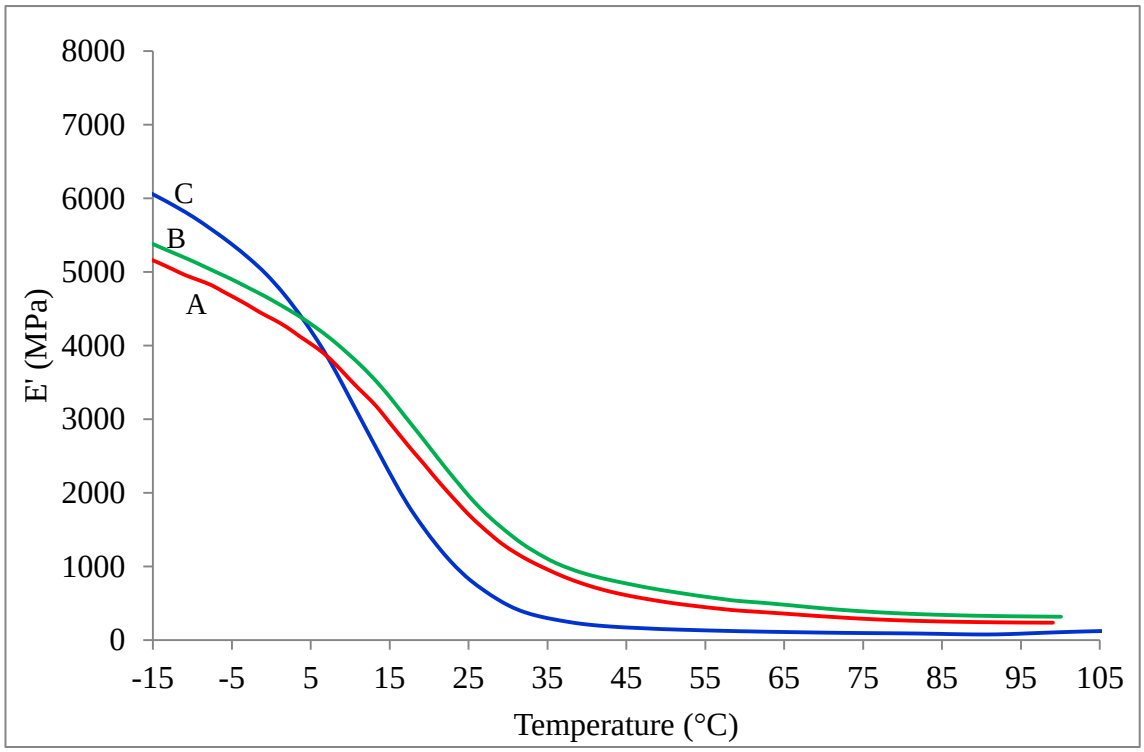

Fig. 4.155 Storage modulus (E') vs. temperature for PVA/1SS/1NP (A) and PVA/1SS/3NP (B) composites. The thermograms were compared with the DMA thermogram for pure PVA (C).

In general, observation on the thermograms revealed that all of the composites of PVA blended with starch and cellulosic fibers exhibit an increase in the storage modulus values when compared to pure PVA over the glass transition temperature region. The E' values also increases with increasing cellulose filler content and this directly indicates that their presence enhanced the stiffness of the PVA/starch matrix. This phenomenon is partly because the reinforcement effect contributed by the cellulosic fibers facilitates the transfer of stress across the interface from PVA and starch to the filler (Yang, Gardner, & Kim, 2009). This also suggests that the bond created between PVA, starch and the cellulose molecules helped store a large amount of elasticity during dynamic loading (Das, et al., 2010). With increasing temperature, pure PVA and the PVA/starch/cellulose fibers blends shows a decreasing storage modulus value. This may be associated with the softening of the matrix polymer at higher temperatures. The softening and flow of the PVA/starch matrix at high temperature is hindered by the presence of fillers and this restriction increases with increasing filler loading. The increased in the storage modulus values also indicates that the composites have higher thermal stability and is attributed by the strong interfacial interaction through hydrogen bonding between large specific surface area of the cellulosic fibers and the PVA/starch matrix (Lu, Weng, & Cao, 2006). Figure 4.156 to 4.159 shows the loss factor versus temperature, as evaluated by DMA measurements in tensile mode for PVA blended with 1g of tapioca starch and mix with different concentration of different treated fibers. Figure 4.160 to 4.163 shows the loss factor versus temperature, as evaluated by DMA measurements in tensile mode for PVA blended with 1g of rice starch and mix with different concentration of different treated fibers. Figure 4.164 to 4.167 shows the storage modulus versus temperature, as evaluated by DMA measurements in tensile mode for PVA blended with 1g of sago starch and mix with different concentration of different treated fibers

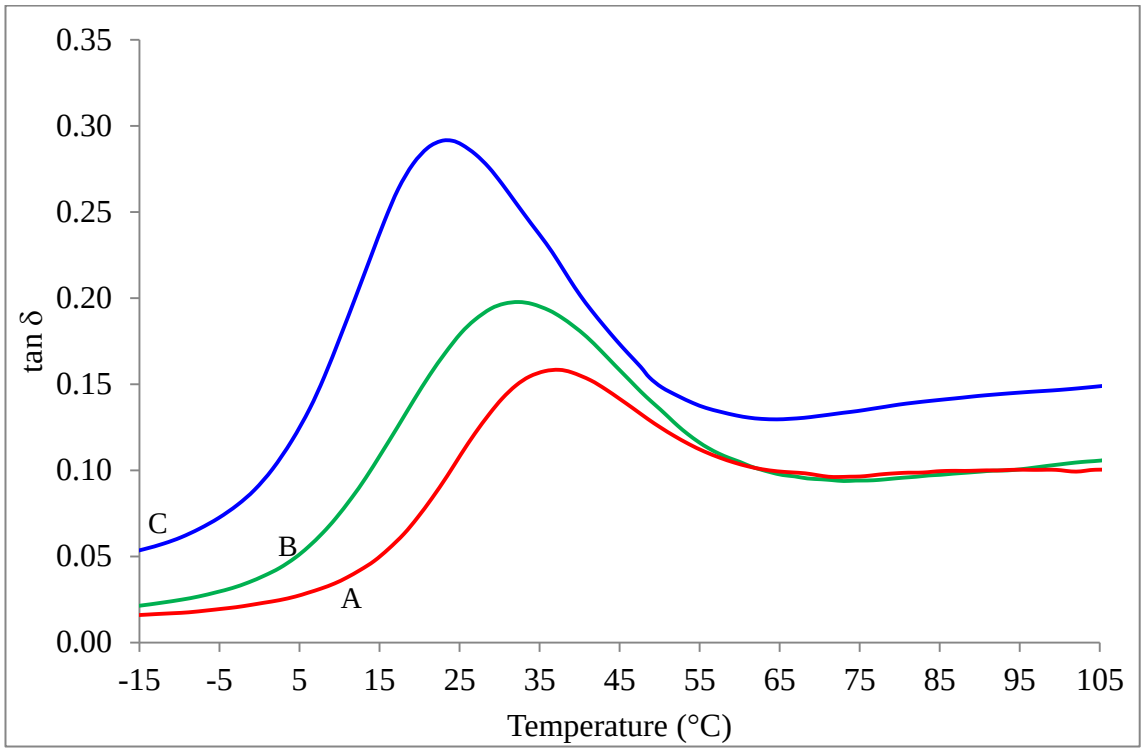

Fig. 4.156 Loss factor (tan δ) vs. temperature for PVA/1TS/1BB (B) and PVA/1TS/3BB (A) composites. The thermograms were compared with the DMA thermogram for pure PVA (C).

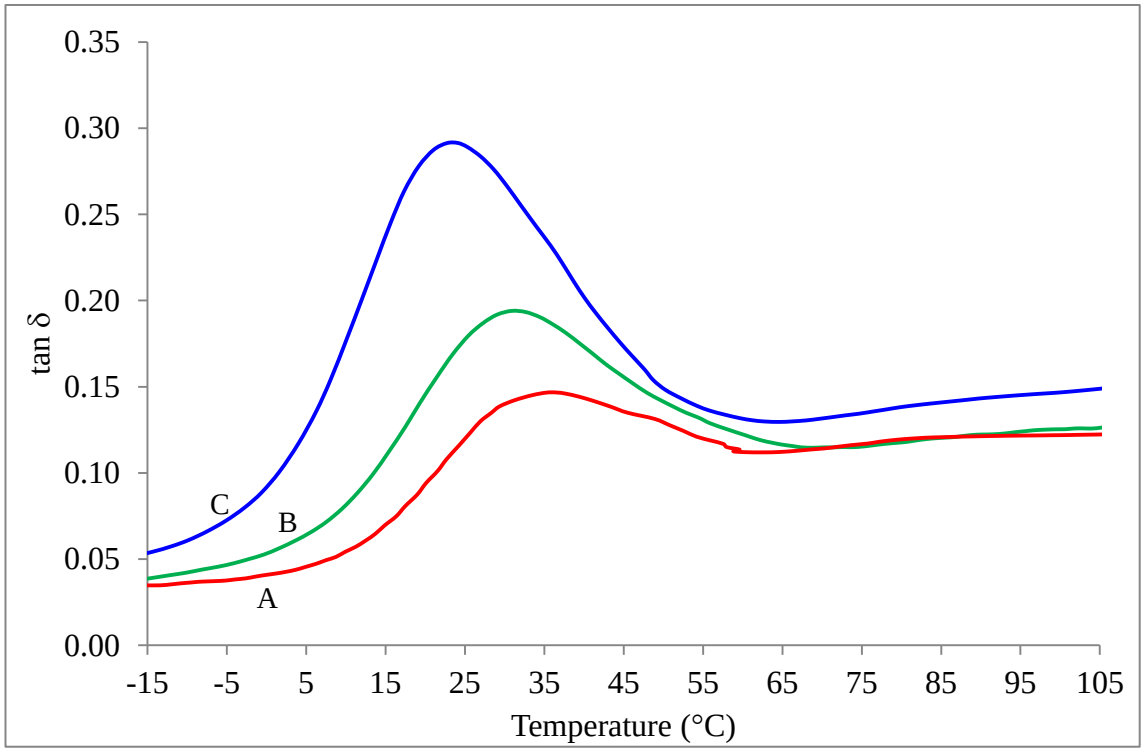

Fig. 4.157 Loss factor (tan δ) vs. temperature for PVA/1TS/1KF (B) and PVA/1TS/3KF (A) composites. The thermograms were compared with the DMA thermogram for pure PVA (C).

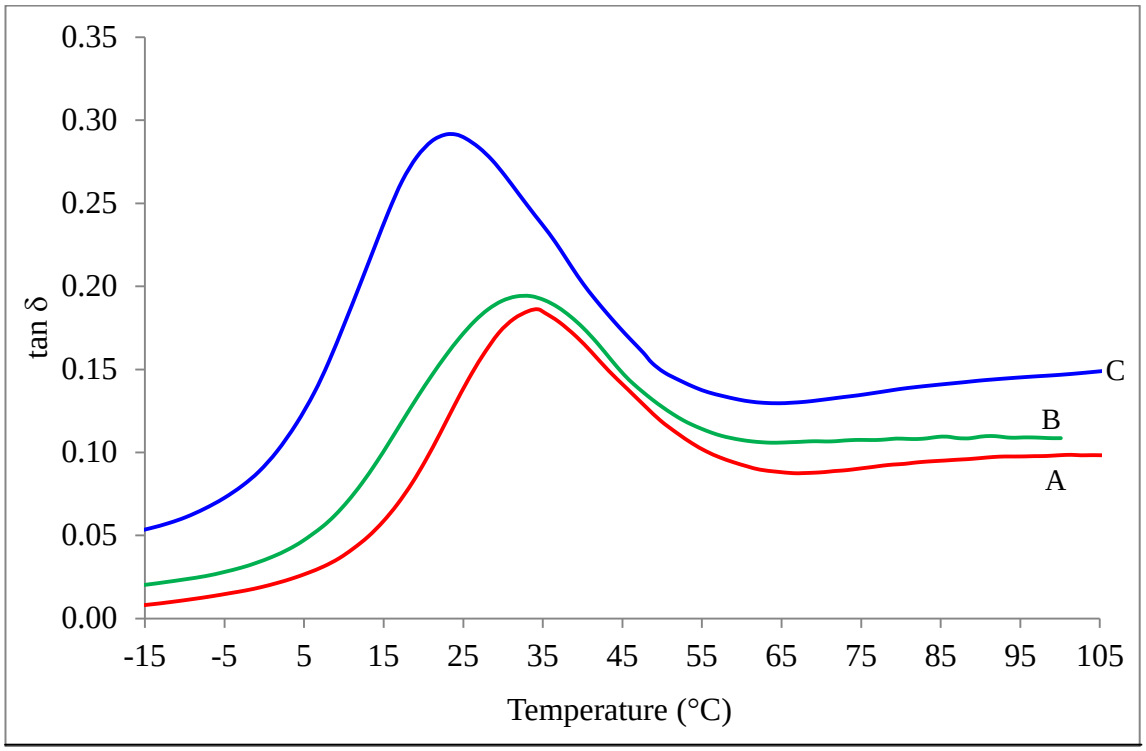

Fig. 4.158 Loss factor (tan δ) vs. temperature for PVA/1TS/1ROS (B) and PVA/1TS/3ROS (A) composites. The thermograms were compared with the DMA thermogram for pure PVA (C).

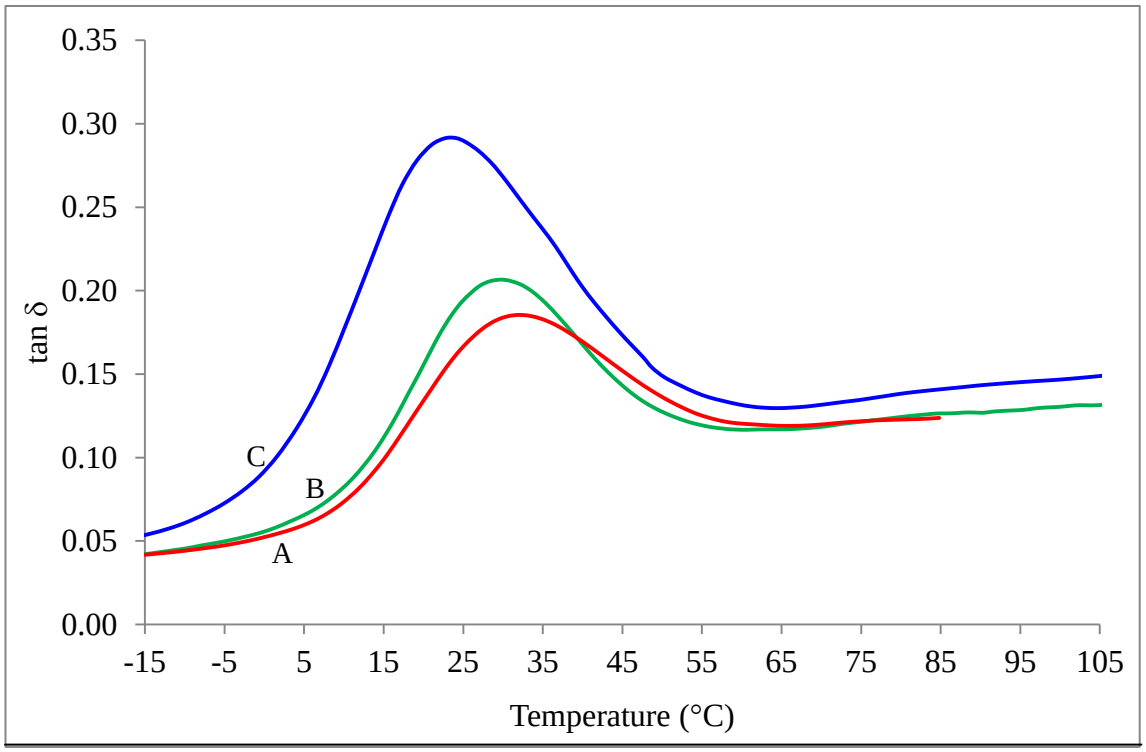

Fig. 4.159 Loss factor (tan δ) vs. temperature for PVA/1TS/1NP (B) and PVA/1TS/3NP (A) composites. The thermograms were compared with the DMA thermogram for pure PVA (C).

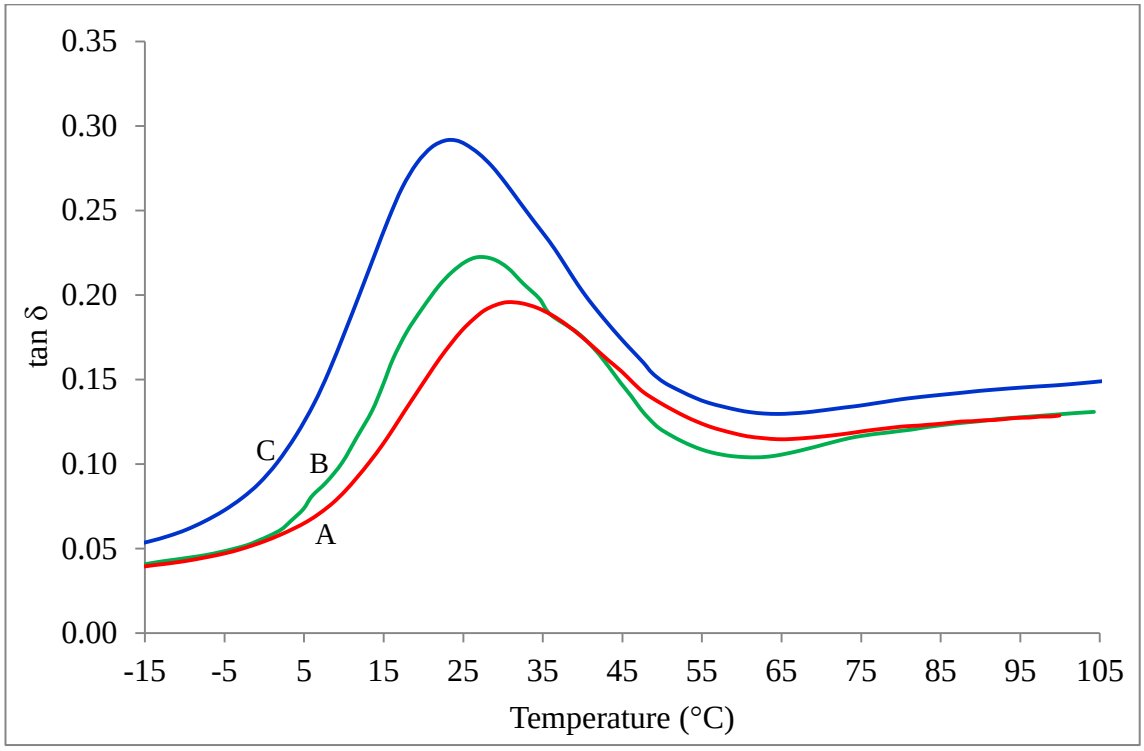

Fig. 4.160 Loss factor (tan δ) vs. temperature for PVA/1RS/1BB (B) and PVA/1RS/3BB (A) composites. The thermograms were compared with the DMA thermogram for pure PVA (C).

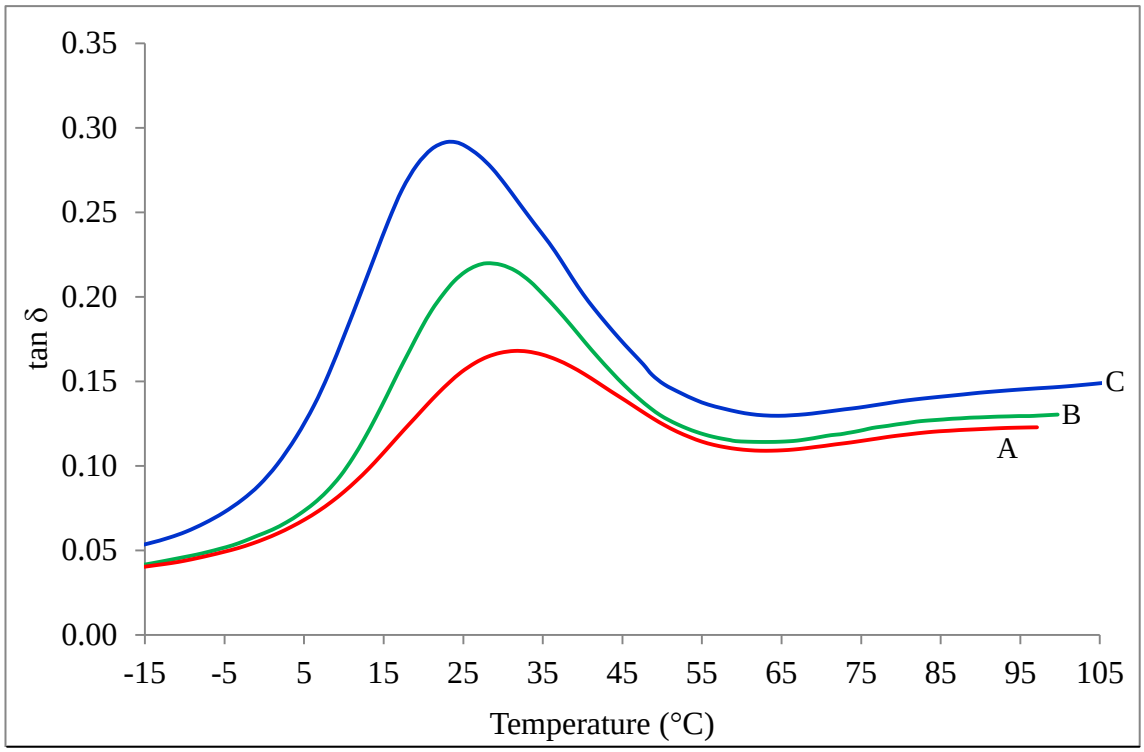

Fig. 4.161 Loss factor (tan δ) vs. temperature for PVA/1RS/1KF (B) and PVA/1RS/3KF (A) composites. The thermograms were compared with the DMA thermogram for pure PVA (C).

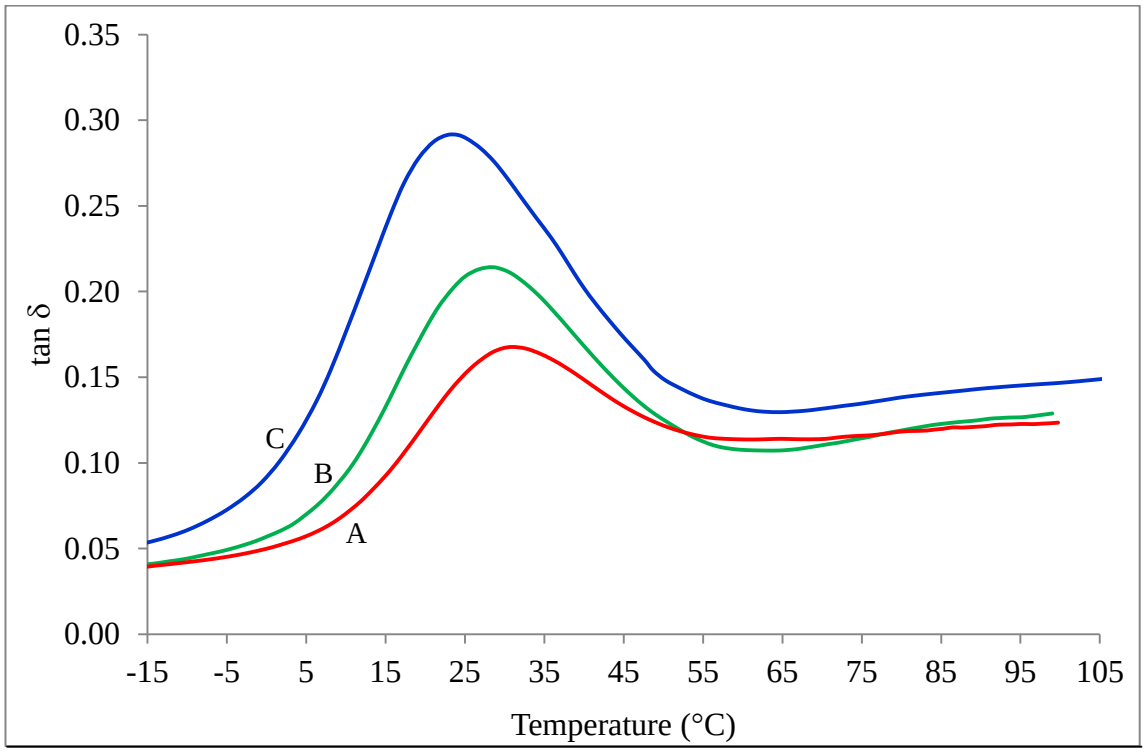

Fig. 4.162 Loss factor (tan δ) vs. temperature for PVA/1RS/1ROS (B) and PVA/1RS/3ROS (A) composites. The thermograms were compared with the DMA thermogram for pure PVA (C)

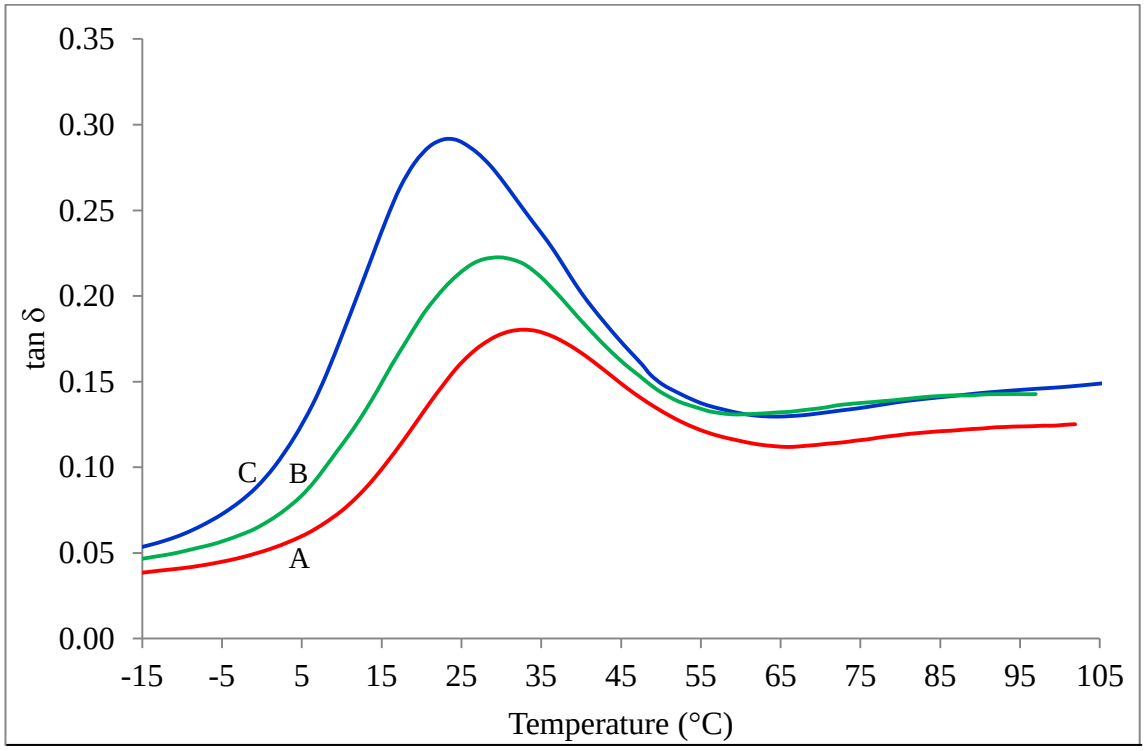

Fig. 4.163 Loss factor (tan δ) vs. temperature for PVA/1RS/1NP (B) and PVA/1RS/3NP (A) composites. The thermograms were compared with the DMA thermogram for pure PVA (C).

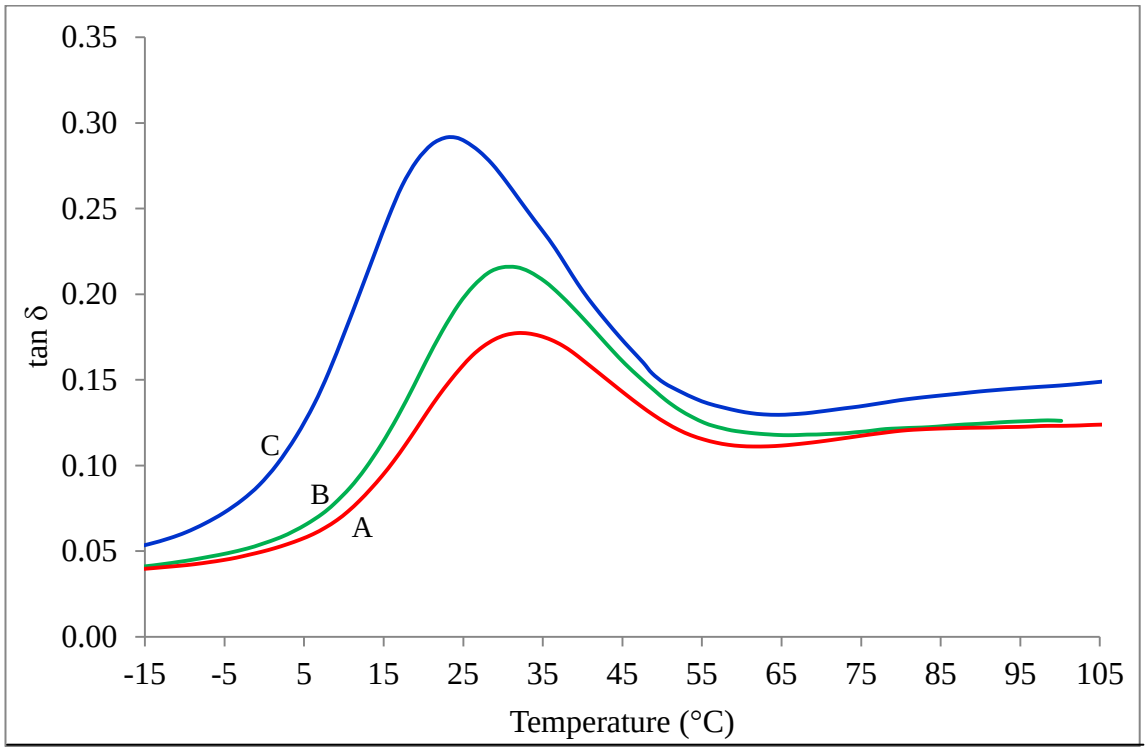

Fig. 4.164 Loss factor (tan δ) vs. temperature for PVA/1SS/1BB (B) and PVA/1SS/3BB (A) composites. The thermograms were compared with the DMA thermogram for pure PVA (C).

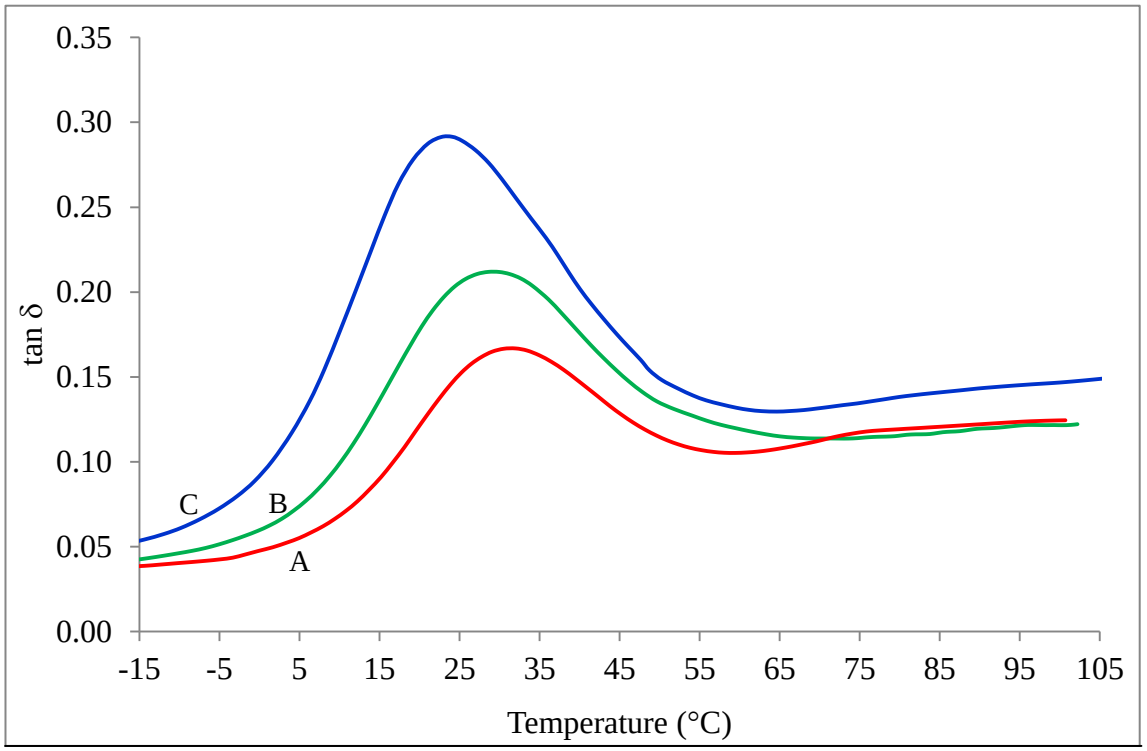

Fig. 4.165 Loss factor (tan δ) vs. temperature for PVA/1SS/1KF (B) and PVA/1SS/3KF (A) composites. The thermograms were compared with the DMA thermogram for pure PVA (C).

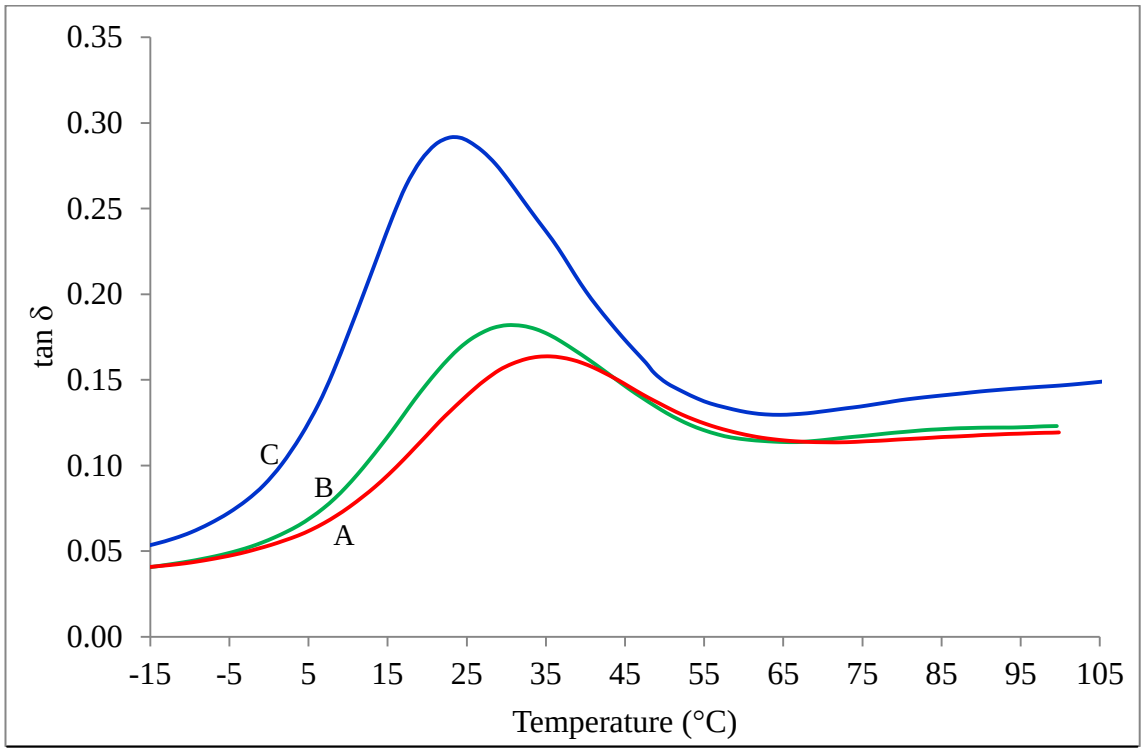

Fig. 4.166 Loss factor (tan δ) vs. temperature for PVA/1SS/1ROS (B) and PVA/1SS/3ROS (A) composites. The thermograms were compared with the DMA thermogram for pure PVA (C)

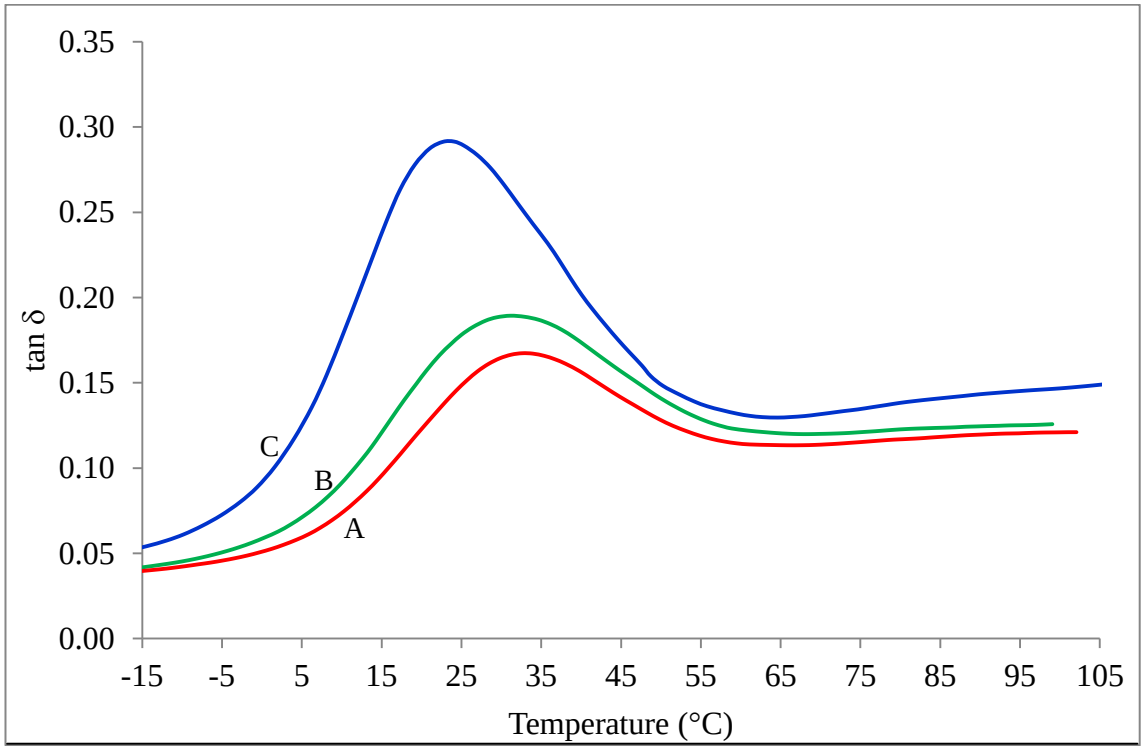

Fig. 4.167 Loss factor (tan δ) vs. temperature for PVA/1SS/1NP (B) and PVA/1SS/3NP (A) composites. The thermograms were compared with the DMA thermogram for pure PVA (C).

The tan δ-temperature curves of the composites show that with increasing cellulosic filler content, the tan δ peak shifts slightly from 24°C to 37°C, indicating that incorporation of the cellulosic fillers inhibits the molecular motion of PVA and starch, and this reaction may be contributed by the strong hydrogen bonding interaction between PVA, starch and the cellulosic fibers. A decrease in the magnitude of the tan δ peaks values of the composite were also noted upon the addition of cellulosic fibers, suggesting that good interfacial interaction exists between the fibers and the polymer/starch matrix. The reason for this behaviour may be due to the interaction that forms a strong network between fiber and matrix that limits the mobility of the polymeric molecular chain in the amorphous portion of the matrix polymers (Corradini, Imam, Agnelli, & Mattoso, 2009). It is also generally observed that the composite of PVA/starch reinforced with fibers also showed a broader peak than pure PVA. The peak gets broader as the concentration of cellulosic content increases. This broadening of the loss modulus peak within the composite may be attributed to the increase in the energy absorption by the fiber therein (Han & Han, 2008). Figure 4.168 and 4.169 shows the storage modulus versus temperature, as evaluated by DMA measurements in tensile mode for PVA blended with different starches and mix with 1g and 3g of treated bamboo fibers, respectively. Figure 4.170 and 4.171 shows the storage modulus versus temperature, as evaluated by DMA measurements in tensile mode for PVA blended with different starches and mix with 1g and 3g of treated kenaf fibers, respectively.

Figure 4.172 and 4.173 shows the storage modulus versus temperature, as evaluated by DMA measurements in tensile mode for PVA blended with different starches and mix with 1g and 3g of treated roselle fibers, respectively. Figure 4.174 and 4.175 shows the storage modulus versus temperature, as evaluated by DMA measurements in tensile

mode for PVA blended with different starches and mix with 1g and 3g of treated napier fibers, respectively.

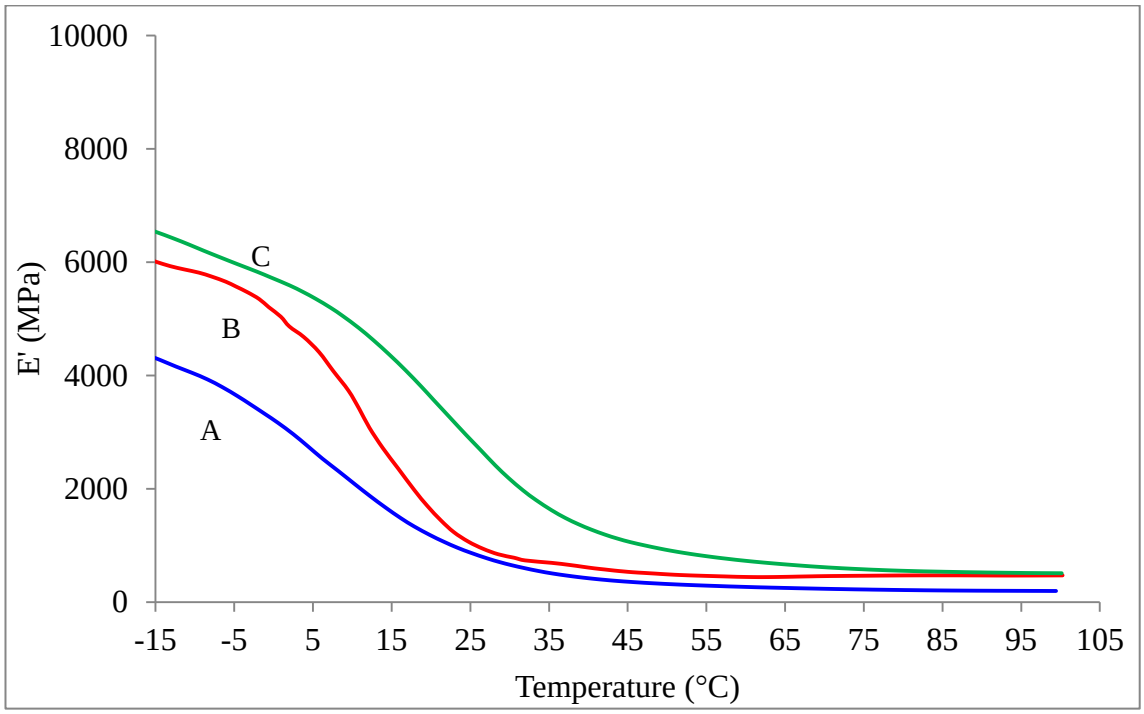

Fig. 4.168 Storage modulus (E') vs. temperature for PVA/1RS/1BB (B), PVA/1TS/1BB (A) and PVA/1SS/1BB (C) composites.

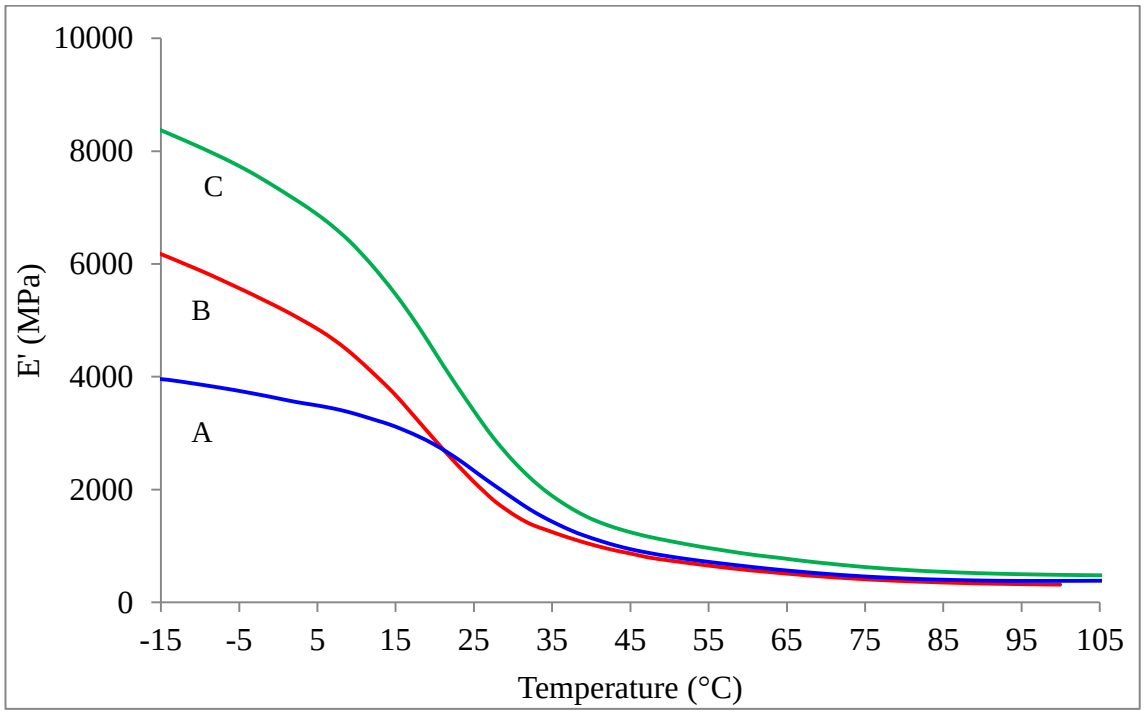

Fig. 4.169 Storage modulus (E') vs. temperature for PVA/1RS/3BB (B), PVA/1TS/3BB (A) and PVA/1SS/3BB (C) composites

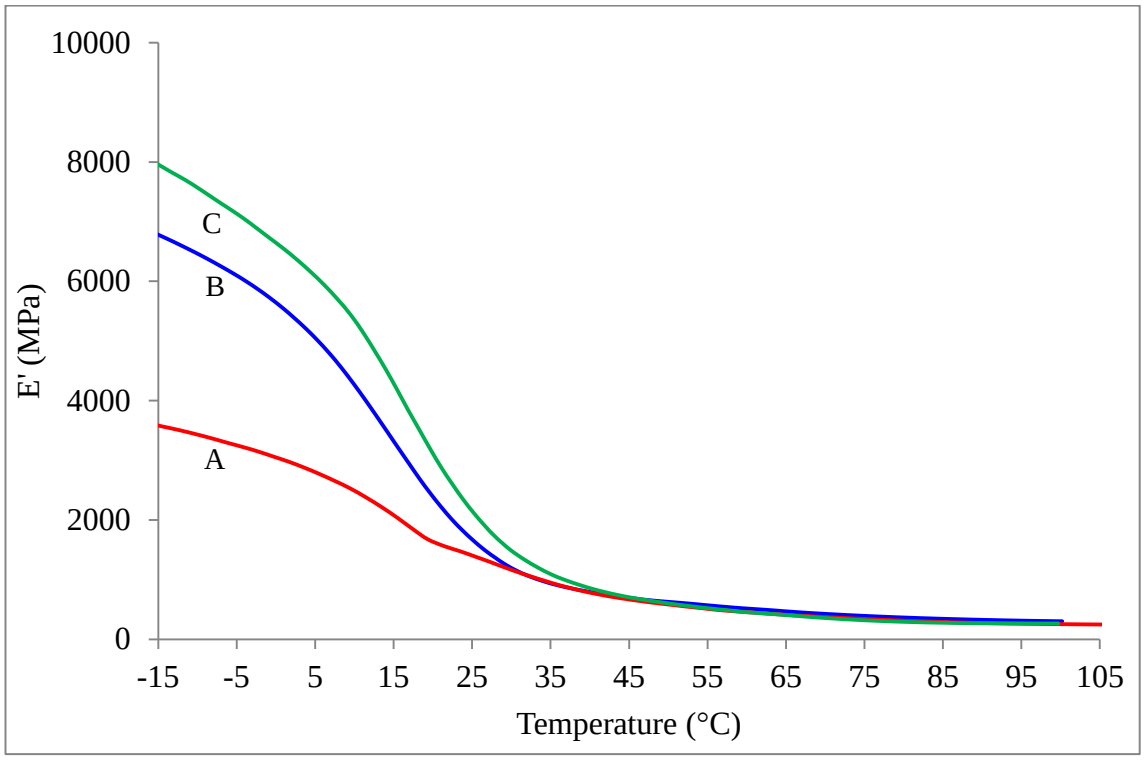

Fig. 4.170 Storage modulus (E') vs. temperature for PVA/1RS/1KF (B), PVA/1TS/1KF (A) and PVA/1SS/1KF (C) composites.

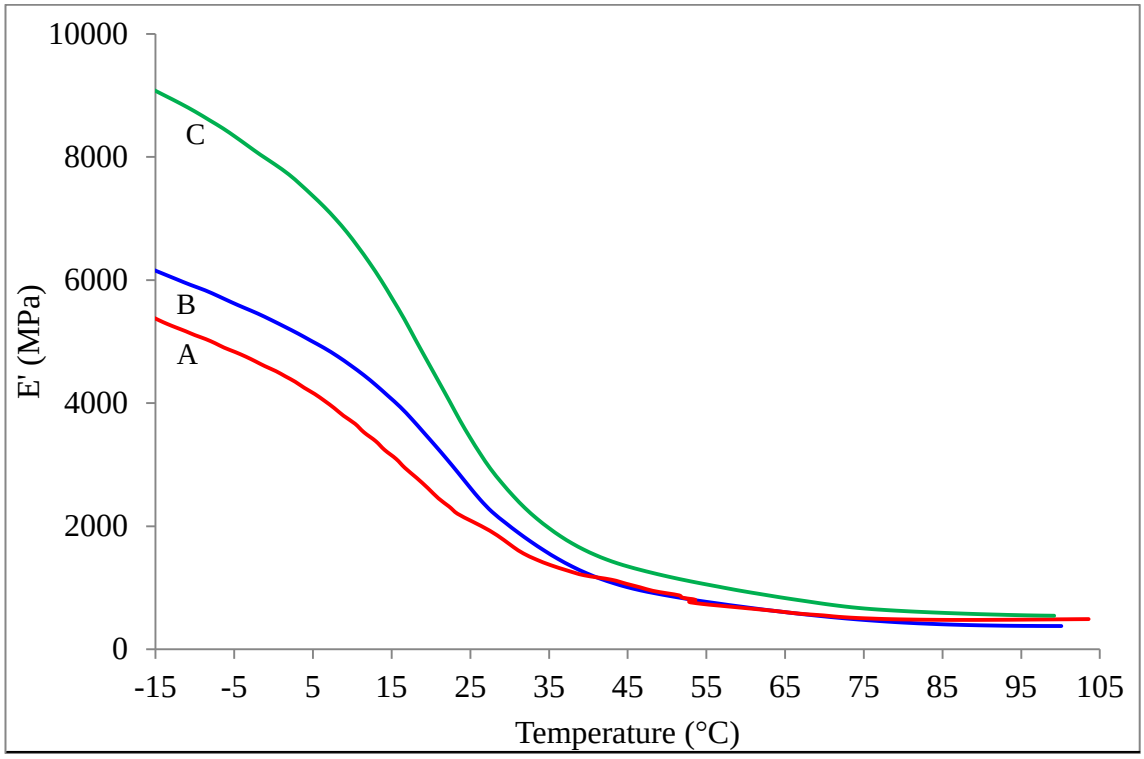

Fig. 4.171 Storage modulus (E') vs. temperature for PVA/1RS/3KF (B), PVA/1TS/3KF (A) and PVA/1SS/3KF (C) composites.

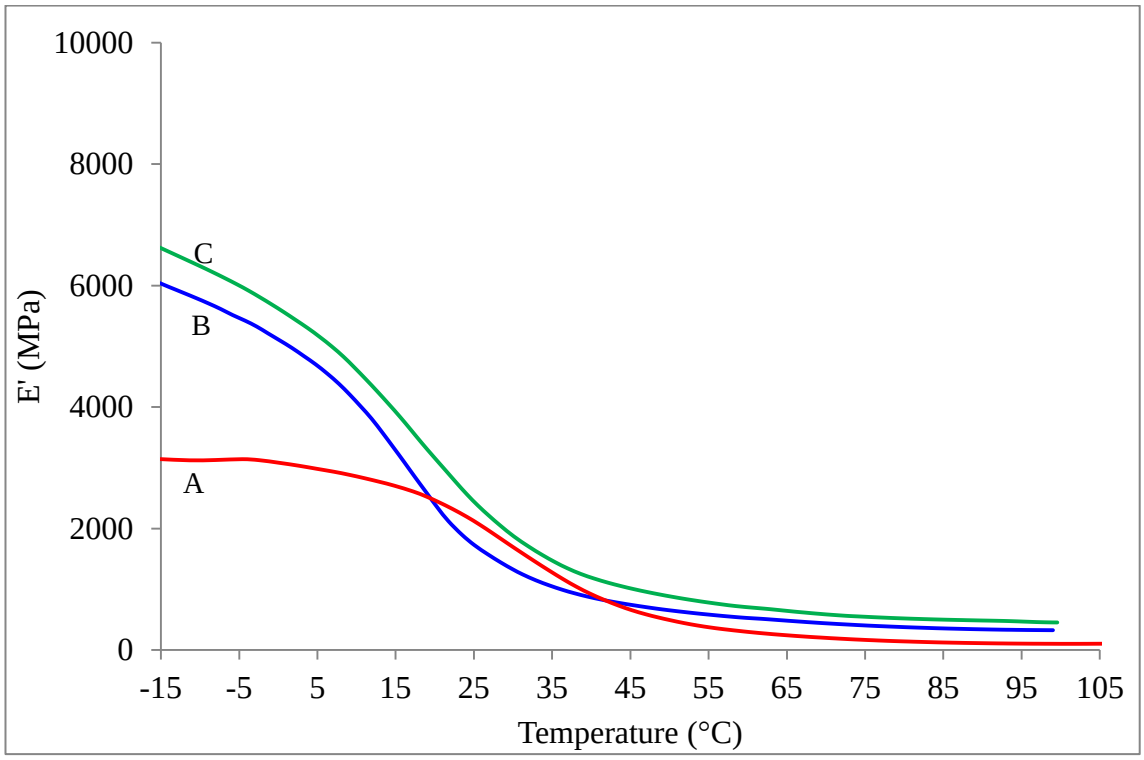

Fig. 4.172 Storage modulus (E') vs. temperature for PVA/1RS/1ROS (B), PVA/1TS/1ROS (A) and PVA/1SS/1ROS (C) composites.

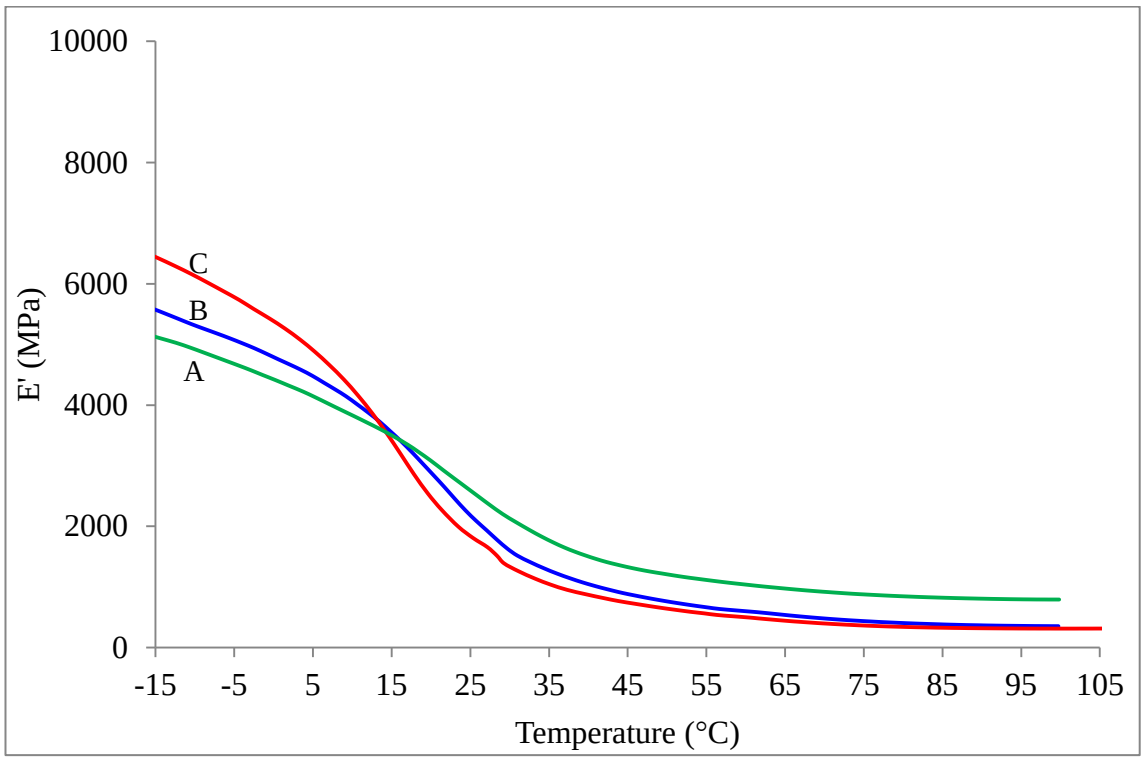

Fig. 4.173 Storage modulus (E') vs. temperature for PVA/1RS/3ROS (B), PVA/1TS/3ROS (C) and PVA/1SS/3ROS (A) composites.

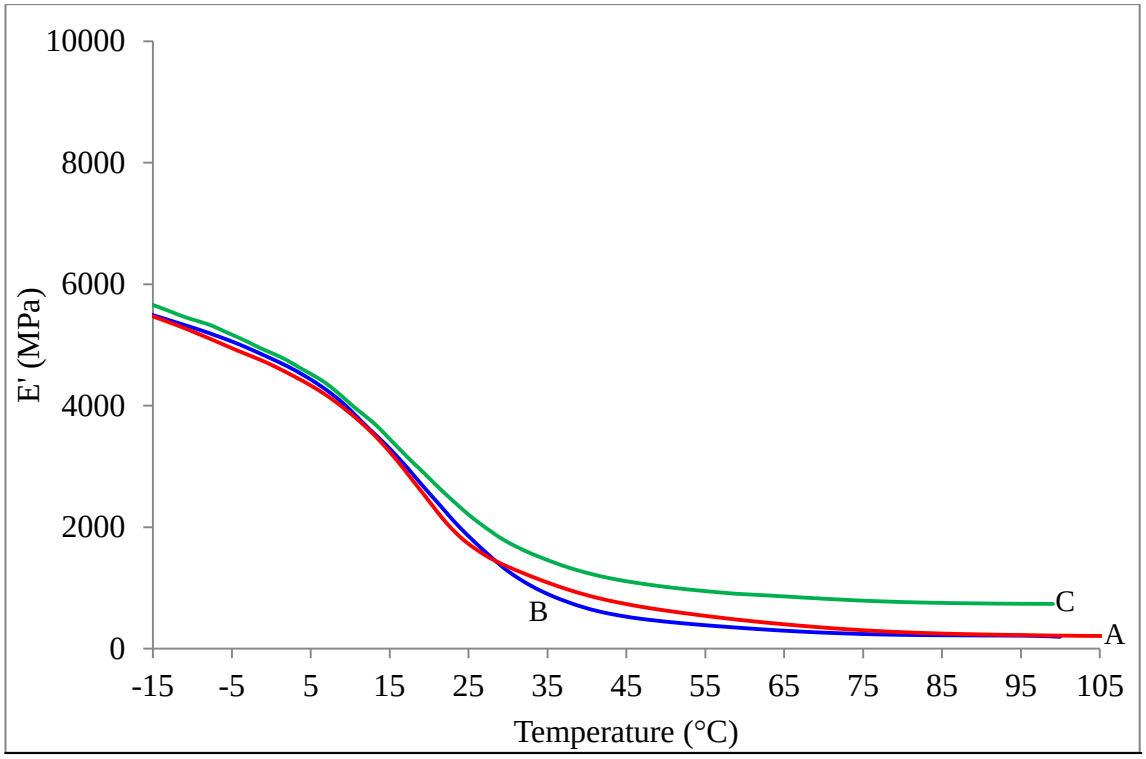

Fig. 4.174 Storage modulus (E') vs. temperature for PVA/1RS/1NP (B), PVA/1TS/1NP (A) and PVA/1SS/1NP (C) composites

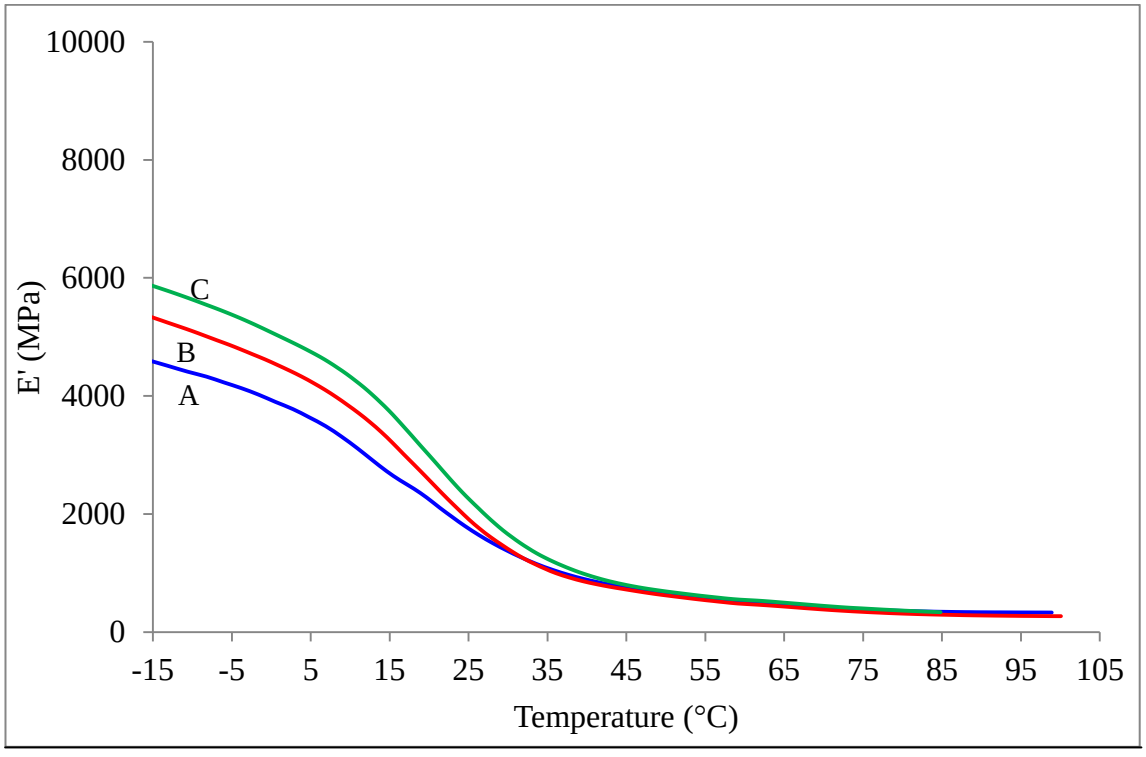

Fig. 4.175 Storage modulus (E') vs. temperature for PVA/1RS/3NP (A), PVA/1TS/3NP (B) and PVA/1SS/3NP (C) composites

From Figures 4.168 to 4.175, the trend projected from the storage modulus values in the in the glass transition region shows that between the PVA/rice/different fibers, PVA/tapioca/different fibers and PVA/sago/different fibers composites, the PVA/sago/different fibers blends exhibited slightly higher E' values. Generally, for a certain composite reinforced with fillers, the higher the storage modulus values are, the higher the mechanical tensile strength and thereby produce a stronger composite (Cho & Park, 2011). These results can be corroborated with the tensile test values for the different composite that will be analyzed in the latter part of this thesis. As it can also be observed that as the content of the cellulose fibers increases in the PVA/sago/different fibers blends, the E' value slightly increases. Conclusively, it can be seen from the figures displayed that the PVA/sago/different fibers composites are slightly superior to its PVA/tapioca/different fibers and PVA/rice/different fibers composites counterpart.